



# Past, present and future rainfall erosivity in Central Europe based on convection-permitting climate simulations

Magdalena Uber<sup>1</sup>, Michael Haller<sup>2</sup>, Christoph Brendel<sup>2</sup>, Gudrun Hillebrand<sup>1</sup>, Thomas Hoffmann<sup>1</sup>

<sup>1</sup>Department Fluvial Morphology, Sediment Dynamics and Management, Federal Institute of Hydrology, 56068 Koblenz, Germany

<sup>2</sup>Deutscher Wetterdienst, 63067 Offenbach am Main, Germany

Correspondence to: Magdalena Uber (uber@bafg.de)

**Abstract.** Heavy rainfall is the main driver of soil erosion by water which is a threat to soil and water resources across the globe. As a consequence of climate change, precipitation -and especially extreme precipitation- is increasing in a warmer world, leading to an increase in rainfall erosivity. However, conventional global climate models struggle to represent extreme rain events and cannot provide precipitation data at the high spatio-temporal resolution that is needed for an accurate estimation of future rainfall erosivity. Convection-permitting simulations (CPS) on the other hand, provide high-resolution precipitation data and a better representation of extreme rain events, but they are mostly limited to relatively small spatial extents and short time periods. Here we present for the first time rainfall erosivity and soil erosion scenarios in a large modelling domain such as Central Europe based on high-resolution CPS climate data generated with COSMO-CLM. We calculate rainfall erosivity for the past (1971-2000), present (2001-2019), near future (2031-2060) and far future (2071-2100) and apply the new data set in the soil erosion model WaTEM/SEDEM for the Elbe River basin. Our results showed that future increases in rainfall erosivity in Central Europe can be up to 84 % in the river basins of Central Europe. These increases are much higher than previously estimated based on regression with mean annual precipitation. In consequence, soil erosion and sediment delivery in the Elbe River basin are also increasing strongly. Locally, changes in erosion rates can be as high as 120 %. We conclude that despite remaining limitations, convection-permitting simulations have an enormous and to date unexploited potential for climate impact studies on soil erosion. Thus, the soil erosion modelling community should follow closely the recent and future advances in climate modelling to take advantage of new CPS for climate impact studies.

## 1 Introduction

Soil erosion by water is one of the main threats to soils worldwide (Amundson et al., 2015; Panagos et al., 2015b). It causes severe ecological and socio-economic problems such as ecosystem degradation (Bilotta and Brazier, 2008; Orgiazzi and Panagos, 2018; Mueller et al., 2020; Stefanidis et al., 2022), loss of fertile topsoil on agricultural land (Pimentel et al., 1995; Zhao et al., 2013; Sartori et al., 2019), channel and reservoir siltation (Wisser et al., 2013; Kondolf et al., 2014) and nutrient and contaminant transport to water bodies (Owens et al., 2005; Ciszewski and Grygar, 2016). Heavy rainfall is the main driving force of soil erosion by water. It acts via the detachment of soil particles by raindrop impact or shear forces of overland flow



and subsequent transport of soil particles with overland flow. Rainfall erosivity is defined as “the capability of rainfall to cause soil loss from hillslopes by water” (Nearing et al., 2017). It is most commonly expressed as the R-factor of the Universal Soil Loss Equation (USLE, Wischmeier and Smith, (1978)) and its revised versions RUSLE (Renard et al., 1993) and RUSLE2 (USDA Agricultural Research Service, 2008). The USLE, its derivatives and models based on the USLE are the most widely  
35 used soil erosion models (Borrelli et al., 2021). The USLE calculates average annual soil loss at a site from rainfall erosivity, soil erodibility, topography, crop management and control practices.

Rainfall erosivity is governed by rainfall kinetic energy, which depends itself on raindrop numbers, sizes and fall velocities (Wilken et al., 2018). As drop size distributions and fall velocity distributions are usually not available for long periods of time and large study sites, rainfall intensity is usually used as a proxy. Numerous kinetic energy - rainfall intensity relations exist  
40 in the literature and are used in soil erosion modelling (Van Dijk et al., 2002; Wilken et al., 2018; Brychta et al., 2022). Thus, site-specific rainfall erosivity expressed as the USLE R-factor is commonly calculated from long lasting precipitation records from rain gauges. R-factor values depend strongly on the temporal resolution of the underlying precipitation data time series. R-factors decrease with decreasing resolution of the precipitation data because intensity peaks are reduced when precipitation is aggregated over longer time spans (Fischer et al., 2018). When high-resolution precipitation data is available only at a few  
45 locations or limited time periods but low-resolution data (daily – annual) is available elsewhere (e.g. denser rain gauge networks, past reconstructions or future projections), so called low-resolution approaches can be applied (Brychta et al., 2022). This approach is based on empirical relations between rainfall erosivity calculated from high-resolution data and lower resolution rainfall amounts (usually monthly, seasonal or annual totals). Application of these approaches to calculate future changes of rainfall erosivity is not permitted if the frequency distribution of rainfall events changes, as expected under climate  
50 change.

Erosion modelling usually requires contiguous data of rainfall erosivity which is highly variable in space (Auerswald et al., 2019a). This spatial variability is usually not represented by rain gauge networks, so spatially interpolated raster data are necessary. Gauge-adjusted radar rainfall data has a high potential for the estimation of highly resolved and contiguous rainfall erosivity maps (Fischer et al., 2018; Risal et al., 2018; Auerswald et al., 2019a; Kreklow et al., 2020). Where ground-based  
55 radar data is not available, satellite-based gridded precipitation data sets can also be used to generate contiguous maps (Vrieling et al., 2010; Teng et al., 2017). However, their errors have to be assessed critically (Phinzi and Ngetar, 2019).

As a result of climate change, precipitation is likely to increase in a warmer world (Sun et al., 2007; Fowler et al., 2021). For Central Europe, a net increase of total precipitation is projected with a decrease in summer and an increase in winter (Brienen et al., 2020; Jacob et al., 2014). Furthermore, extreme precipitation is increasing in an intensified hydrologic regime under  
60 climate change in many parts of the world as well as in Central Europe. This is due to the fact that the share of convective precipitation in total precipitation is increasing (Berg et al., 2013). Trends of an increase in the frequency and intensity of extreme precipitation have been observed since the beginning of the 20<sup>th</sup> century (Groisman et al., 2005; Alexander et al., 2006; Arnone et al., 2013; Kendon et al., 2014; Fischer and Knutti, 2016) and are expected to continue in the future (Allen and Ingram, 2002; Kharin et al., 2013; Scoccimarro et al., 2013; Westra et al., 2013; Westra et al., 2014; Kendon et al., 2017;



65 Fowler et al., 2021). Thus, rainfall erosivity and soil erosion are also observed to increase and expected to increase further  
(Nearing et al., 2004; Mueller and Pfister, 2011; Hanel et al., 2016a; Panagos et al., 2017; Panagos et al., 2022; Auerswald et  
al., 2019a; Auerswald et al., 2019b; Borrelli et al., 2020).

For climate impact studies on soil erosion, a common limitation is the lack of reliable high-resolution precipitation data for the  
future (Eekhout and De Vente, 2020). Projections of future precipitation from regional climate models in Europe are typically  
70 available at a temporal resolution of one day and a spatial resolution of  $0.11^\circ$  (approx. 12 km) (e.g. Jacob et al., 2014). Thus,  
low-resolution approaches based on regression models that estimate future R-factors from monthly or annual precipitation are  
commonly applied (Eekhout and De Vente, 2020). Out of 68 climate impact assessment studies reviewed by Eekhout and De  
Vente (2020) only four used sub-daily precipitation data. In the review of 3030 soil erosion modelling studies by Borelli et al.  
(2021), 196 were identified to have the aim to model “climate change” or “Land use change and climate change” impacts.  
75 Only 11 studies are quoted to use sub-daily precipitation data. The few studies that use hourly or sub-hourly future precipitation  
data mostly use either statistical downscaling of lower resolution data (Routschek et al., 2015; Wang et al., 2018) or artificially  
generated precipitation time series (e.g. Coulthard et al., 2012; Simonneaux et al., 2015). Strictly speaking, regression-based  
models applying monthly or annual precipitation are only valid for the time period for which these models are calibrated and  
lead to underestimations of the rainfall erosivity if extreme precipitation events increase with time, as suggested by many  
80 climate change scenarios.

Only recently, the development of convection-permitting climate simulations (CPS) offers the possibility to model rain  
erosivity considering the effects of changing frequency of heavy precipitation that predominantly drives future soil erosion.  
Thus, CPS have an enormous and to date unexploited potential for the calculation of future rainfall erosivity. Usually,  
convection-permitting means that the standard parametrization of convective rainfall is switched off in the model setup,  
85 allowing the model to simulate the precipitation explicitly in each grid cell. As the grid size of most CPS still ranges between  
2 and 4 km, large deep convection cells are explicitly simulated, while smaller shallow convection still needs to be simulated  
using a parametrization. Despite this shortcoming, CPS provide an improved representation of extreme precipitation compared  
to climate models with parametrized deep convection. This is due to several improvements: the diurnal cycle is strongly  
improved (Ban et al., 2014; Prein et al., 2015; Haller et al., 2023), the return periods of extreme precipitation are better  
90 represented (Rybka et al., 2022) and added value diagnostics have been applied for the comparison to coarse climate model  
data (Raffa et al., 2021; Haller et al., 2023). However, CPS also show some limitations. The simulations on the km-scale for  
regional domains are still time-consuming and they need a considerable amount of computing power. Compromises have to  
be made: either the covered time period is shortened or the model domain is restricted to the region of interest. Up to some  
years ago, only single CPS have been performed, covering only one future scenario. Thus, given the novelty of CPS, model  
95 ensembles are not yet available for regional model domains, at the time scales needed for the robust estimation of rainfall  
erosivity ( $\sim 20$  years) or for several emission scenarios. Lately, the first-of-its-kind CPS ensembles have been created through  
combined efforts in the CPS community (Coppola et al., 2020; Ban et al., 2021). Even though these ensemble simulations do



not cover the long time periods needed for the estimation of rainfall erosivity yet, these flagship studies show promising results that suggest that in the future ensembles of CPS will be available for climate impact studies including studies on soil erosion.

100 The COSMO-CLM is a regional climate model that is used on horizontal scales from 1 to 50 km (Rockel et al., 2008). It is the climate version of the former operational forecast model COSMO of the German meteorological service (Deutscher Wetterdienst, DWD) and other European partners. COSMO-CLM is jointly maintained and developed by the CLM-Community but will soon be gradually replaced by the newly developed model ICON-CLM (Pham et al., 2021). In the framework of the project BMDV-Expertennetzwerk, convection-permitting climate simulations have been performed with

105 COSMO-CLM. Three time periods including one historical period (1971-2000, called CPS-hist) and two future periods (CPS-scen; near future: 2031-2060; far future: 2071-2100) were simulated by dynamically downscaling from global model data. Additionally, evaluation simulations were conducted with reanalysis data forcing for the time period 1971-2019 (CPS-eval). The data are published and usable for manifold analyses and impact model studies.

The improved representation of extreme precipitation in CPS compared to conventional convection-parametrized climate

110 models as well as the high spatio-temporal resolution of CPS is of great benefit for climate impact studies in soil erosion modelling (Chapman et al., 2021). Using CPS with high temporal resolution facilitates the direct calculation of the R-factor and avoids the application of regression equations between the R-factor and annual precipitation, which are established for past climates but may not be valid for future climate with different precipitation frequency and magnitude. To our knowledge, to date only one study (Chapman et al., 2021) assessed the impact of climate change on soil erosion using a convection-

115 permitting climate model. They used 15-min precipitation data from the pan-African model CP4A to calculate rainfall erosivity in Tanzania and Malawi for 8 years in the past and 8 years in the future. Their results suggested that convection-parameterized regional and global climate models might underestimate future rainfall erosivity while CPS represent observed storm characteristics better. Nonetheless, there are remaining limitations of CPS that hinder their use in soil erosion modelling:

- i) limited spatial extent of most CPS. While regional and global convection-parameterized simulations cover the entire

120 globe, to date CPS are only available for some regions.

- ii) the relatively short periods of time covered by CPS. Because of the high interannual variability of rainfall erosivity, long time series are required for robust estimates of long-term R-factors. Wischmeier et al. (1958) give a minimum of 20 years.
- iii) the lack of model ensembles. While ensembles of regional or global climate models give more robust estimates of

125 the future climate than single ensemble members, ensembles of CPS are only being developed recently.

Covering an area of approx. 1.6 million km<sup>2</sup> on land and in total 109 years, the CPS performed at DWD with COSMO-CLM overcome the limitations i) and ii) for the first time and are thus a valuable source of precipitation data for the estimation of rainfall erosivity in Central Europe.

In this study, we calculated rainfall erosivity in Central Europe expressed as the USLE R-factor for the past (1971-2000),

130 present (2001-2019), near future (2031-2060) and far future (2071-2100) from convection-permitting climate model output.



We assessed changes in rainfall erosivity from the climate model output for a historical and future time period. Furthermore, a first application of the new rainfall erosivity maps is presented. To this end, changes in soil erosion and sediment delivery to the Elbe River are modelled in the USLE-based model WaTEM/SEDEM. Finally, we discuss the potential and limitations of using CPS for the calculation of rainfall erosivity. The main remaining limitation is the fact that to date ensembles of CPS do not exist yet at time scales covering at least 20 years needed for robust rainfall erosivity estimations. In consequence, the uncertainty due to the choice of the model and the emission scenario cannot be assessed. To address this problem, we compare or results to the ones obtained from an ensemble of conventional regional climate models as well as to results from the literature. To our knowledge, this is the first test case that applies CPS for the calculation of rainfall erosivity and soil erosion covering national spatial scales and temporal scales in the order of 30 years.

## 140 2 Material and methods

### 2.1 COSMO-CLM

Convection-permitting simulations were conducted using the non-hydrostatic regional climate model COSMO-CLM. It shares almost all relevant modules with the weather forecast model COSMO (Doms et al., 2001), which has been the operational weather forecast model of DWD for more than a decade, before it was replaced by the ICON model (Giorgetta et al., 2018) in recent times. COSMO-CLM, the climate version of COSMO, is optimized for long-term climate runs for more than 15 years (Rockel et al., 2008; Sorland et al., 2021). The general COSMO characteristics (e.g. physics) are documented in Steppeler et al. (2003). The COSMO-CLM is described in more detail in Böhm et al. (2006). COSMO-CLM is usable on different horizontal grid widths and has a typical vertical spacing of 50 layers in the troposphere and the lower stratosphere up to about 22 km. Subgrid-scale physical processes are parametrized, as they cannot be calculated explicitly. For grid spacings of less than 4 km, the convection parametrization scheme for deep convection is turned off, while the shallow convection scheme remains turned on. In the COSMO-CLM standard parametrization for coarser grid resolutions, both parts are switched on. The model domain of the CPS has 415 x 423 grid points and is centred over Germany. It includes large parts of neighbouring countries and therefore fully covers the contributing catchment areas of the major Central European rivers Rhine, Elbe, Oder and Upper Danube until Bratislava (Fig. 1). The grid resolution is  $0.0275^\circ$  ( $\approx 3$  km). The model uses the standard parametrizations for turbulence and (shallow) convection as well as for the time integration.

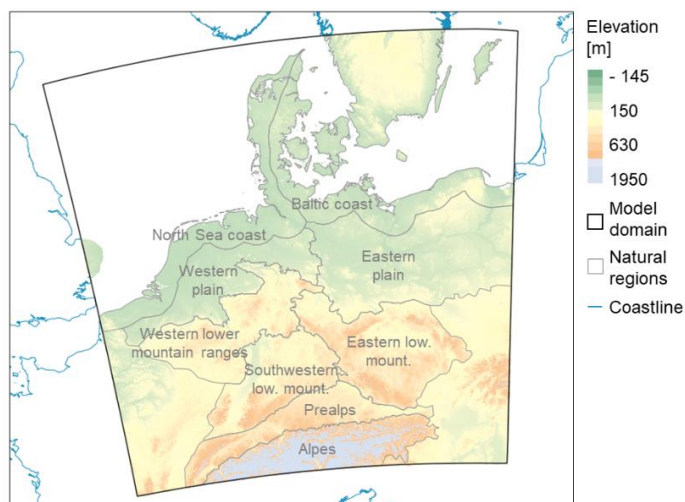


**Figure 1: Extent of the CPS model domain. Colours show the elevation (source: EU-DEM, Copernicus Land Monitoring Service, 2016). The natural regions outlined in grey were adapted from Bundesamt für Naturschutz (2017).**

For the projection simulations, three 30-year time slices have been selected, covering the years 1971-2000 (historical, CPS-hist) and 2031-2060/2071-2100 (scenario, CPS-scen). CMIP5 global model data from the MIROC-MIROC5 (Watanabe et al., 2010) have been dynamically downscaled, applying the RCP8.5 scenario. The downscaling has been performed using an intermediate nesting step of 12 km.

The CPS evaluation simulation (CPS-eval) covering the time range of 1971–2019 is driven by ERA5 (Hersbach et al., 2020) for the years 1979 to 2019 and by ERA-40 reanalysis data (Uppala et al., 2005) for the years 1971 to 1978. ERA5 and ERA40 are reanalysis data that provide a comprehensive and coherent information of essential climate variables by assimilating additional various observational data to a model grid. The model system itself remains unchanged throughout the entire time period, resulting in a consistent approach to data assimilation and various parameterizations. For the ERA-40-driven time period, we used a two-fold nesting with a middle step at  $0.11^\circ$ , while for the ERA5-driven time period, a direct downscaling from 30 to 3 km was applied.

The model output consists of hourly data for the most important variables (e.g. temperature, precipitation, humidity and wind). It is available at <https://esgf.dwd.de/projects/dwd-cps/> (accessed 10 February 2023) (Brienen et al., 2022; Haller et al., 2022a, b). The overall configuration of our simulation has been taken from the joint FPS-convection contribution in the CLM-community (Coppola et al., 2020). The hourly precipitation data that was further processed for this study was organized in five data sets, i.e. the projection simulations for the historical period, the near and far future (CPS-hist, CPS-scen-nf, CPS-scen-ff) as well as the evaluation simulations for the historical period and the present (CPS-eval-hist, CPS-eval-present).



## 2.2 Calculation of rainfall erosivity

### 2.2.1 High temporal resolution approach

Following Wischmeier and Smith (1958; 1978) and Wischmeier (1959), the erosivity of an erosive rain event  $R_e$  [ $N h^{-1}$ ] is calculated as the product of maximum 30 min rain intensity  $I_{max30}$  [ $mm h^{-1}$ ] and kinetic energy  $E_{kin}$  [ $kJ m^{-2}$ ] of the rain event:

$$180 \quad R_e = I_{max30} * E_{kin} \quad (1)$$

An erosive rain event is defined as having a total precipitation (P) of at least 12.7 mm or a maximum 30 min rainfall intensity ( $I_{max30}$ ) of at least 12.7  $mm h^{-1}$  and at least 6 h separate two erosive rain events. We use the classical equation by Wischmeier and Smith (1978) to calculate kinetic energy based on high-resolution rainfall data. Transferred to SI units, it calculates specific kinetic energy per millimeter rain depth,  $e_{kin,i}$  in  $kJ m^{-2} mm^{-1}$  for every time increment during an erosive rainfall event as follows (Rogler and Schwertmann, 1981):

$$185 \quad e_{kin,i} = \begin{cases} 0 & \text{for } I < 0.05 \text{ mm h}^{-1} \\ (11.89 + 8.73 * \log_{10} I) * 10^{-3} & \text{for } 0.05 \text{ mm h}^{-1} \leq I < 76.2 \text{ mm h}^{-1} \\ 28.33 & \text{for } I \geq 76.2 \text{ mm h}^{-1} \end{cases} \quad (2)$$

To obtain  $E_{kin}$  for each event,  $e_{kin,i}$  is multiplied with rain depth of each timestep and summed up for the entire rain event. Annual rainfall erosivity of a specific year is obtained by summing up  $R_e$  of all erosive rain events in that year. The USLE R-factor is the long-term average of annual rainfall erosivity. R-factors are often given in the unit  $MJ mm ha^{-1} h^{-1} a^{-1}$ . To convert rainfall erosivity as given here in  $N h^{-1} a^{-1}$  to  $MJ mm ha^{-1} h^{-1} a^{-1}$ , it has to be multiplied with a factor 10.

Here we calculated annual erosivity as well as long-term average annual erosivity for each one of the 175,545 grid points and for each of the five data sets (CPS-hist, CPS-scen-nf, CPS-scen-ff, CPS-eval-hist, CPS-eval-present). We used the command line suite Climate Data Operators (CDO, Schulzweida, 2022) and the library ncdf4 (Pierce, 2019) of the statistical software R to extract time series of 30 years (19 years for CPS-eval-present) for each grid cell and each data set and calculated rainfall erosivity as described above. As the COSMO-CLM model output is available at a temporal resolution of 60 min, three adjustments were made as proposed by Fischer et al. (2018): (i) the rainfall intensity threshold of  $I_{max30}$  to define an erosive rain event was lowered from 12.7  $mm h^{-1}$  to 5.8  $mm h^{-1}$ , (ii)  $I_{max30}$  in Eq. (1) was replaced by maximum 60 min rainfall erosivity  $I_{max60}$  and (iii) a temporal scaling factor of 1.9 was applied to the R-factor for Germany to account for the reduction of intensity peaks with lower temporal resolution data. Here we did not apply a spatial scaling factor because it is unclear if such a modification is necessary for climate model output.

We further assessed the seasonal distribution of erosivity by calculating the erosion index for each day of the year. The erosion index gives the contribution of each day to annual erosivity. The seasonal distribution of erosivity is important for soil erosion assessments, because of its interactions with seasonal changes of the crop cover. Briefly, high rainfall erosivity in months where vegetation cover is scarce (in Central Europe the winter months) is more severe than high rainfall erosivity during the vegetation period (i.e. the summer months). The erosion index was calculated for each one out of 175,545 grid points and each



day of each year and averaged over all grid points and all 30 years in the three data sets from the projection simulations (CPS-hist, CPS-scen-nf, CPS-scen-ff).

### 2.2.2 Low temporal resolution approach

For comparison, we also calculated rainfall erosivity ( $R$ ) for the past (1971-2000), near future (2031-2060) and far future  
210 (2071-2100) from mean annual precipitation (MAP). Therefore, we used the empirical regression equation

$$R [N h^{-1} a^{-1}] = 0.0788 * MAP [mm] - 2.82 \quad (3)$$

from the German norm DIN 19708 (Din-Normenausschuss Wasserwesen, 2017), which was derived from regression analysis  
of  $R$ -factor values calculated based on Eq. (1) and annual precipitation sums for the time period from the 1960s to the 1980s  
in Germany. We used the median of the MAP of a climate model ensemble consisting of 21 members that were run with the  
215 emission scenario RCP 8.5. The models are part of the DWD reference ensemble ([www.dwd.de/ref-ensemble](http://www.dwd.de/ref-ensemble), accessed on 20  
October 2022).

### 2.3 Soil erosion modelling of the Elbe River basin

To study the effects of changing rainfall erosivity on soil erosion, we used the Water and Tillage Erosion Model and Sediment  
Delivery Model (WaTEM/SEDEM, Van Oost et al., 2000; Van Rompaey et al., 2001; Verstraeten et al., 2002) that was already  
220 applied to the Elbe River basin by the authors of this study (Uber et al., 2022). The Elbe River is one of the largest rivers in  
Central Europe and its basin has a size of 148,300 km<sup>2</sup> located mainly in Germany and the Czech Republic (ICPER, 2016).  
Erosion rates are highest in the central part of the catchment on agricultural areas in rolling terrain (Pohlert, 2015; Uber et al.,  
2022). Locally, simulated erosion rates can be as high as 0.2 mm a<sup>-1</sup> (Uber et al., 2022). The average annual suspended sediment  
load at the most downstream monitoring station at Hitzacker is approximately 600 kt a<sup>-1</sup>. Contaminated legacy sediments from  
225 industry and mining as well as present-day sediment contamination from diffuse and point sources are major threats for the  
water quality of the Elbe River (ICPER, 2014). Furthermore, in the Lower Elbe, the estuary and the German Bight,  
eutrophication and oxygen depletion impair the water quality (Bergemann et al., 1996; Schöl et al., 2014; OSPAR Commission,  
2017; Ritz and Fischer, 2019). Thus, the goal of a good ecologic status set by the European Water Framework Directive is not  
accomplished (ICPER, 2014). A further problem is the deposition of fine sediments in zones of low flow where dredging is  
230 necessary. The waste management of the usually contaminated dredged material is very expensive (ICPER, 2014).

WaTEM/SEDEM calculates average annual soil erosion  $E$  [kg m<sup>-2</sup> a<sup>-1</sup>] based on the USLE:

$$E = R \times K \times LS \times C \times P \quad (4)$$

where  $R$  is the rainfall erosivity factor [MJ mm m<sup>-2</sup> h<sup>-1</sup> a<sup>-1</sup>],  $K$  is the soil erodibility factor [kg h MJ<sup>-1</sup> mm<sup>-1</sup>],  $LS$  is the slope  
length factor [-],  $C$  is the crop factor [-] and  $P$  is the erosion control practice factor [-]. Downslope sediment transport is  
235 simulated with a transport capacity (TC) approach which calculates TC [kg m<sup>-1</sup> a<sup>-1</sup>] as:





$$TC = k_{TC} \times R \times K (LS - 4.08s^{0.8}) \quad (5)$$

where  $k_{TC}$  is a transport capacity coefficient [m] and  $s$  is the slope gradient [ $m\ m^{-1}$ ].  $k_{TC}$  has to be calibrated. For each grid cell, it is determined whether TC exceeds the erosion rate plus possible input from neighboring cells. If this is the case, all eroded particles get transported downstream. If this is not the case, the difference gets deposited at the respective cell.

240 The soil erodibility factor  $K$  was taken from Panagos et al. (2014). The slope length factor was calculated with the Algorithm by McCool et al. (1989) from the digital elevation model EU-DEM of the European Environment Agency (Copernicus Land Monitoring Service, 2016), which was aggregated to a resolution of 100 m. The crop factor was obtained via reclassification of the Corine Land Cover data (Copernicus Land Monitoring Service, 2019) using the crop factor values for different land use classes given by Panagos et al. (2015a). Because no information on erosion control practices is available, the  $P$  factor was set  
245 to one in the entire catchment. In this study, we aim at identifying the impact of climate change; thus, only changes in the  $R$ -factor are considered while changes in future land use are not considered here.

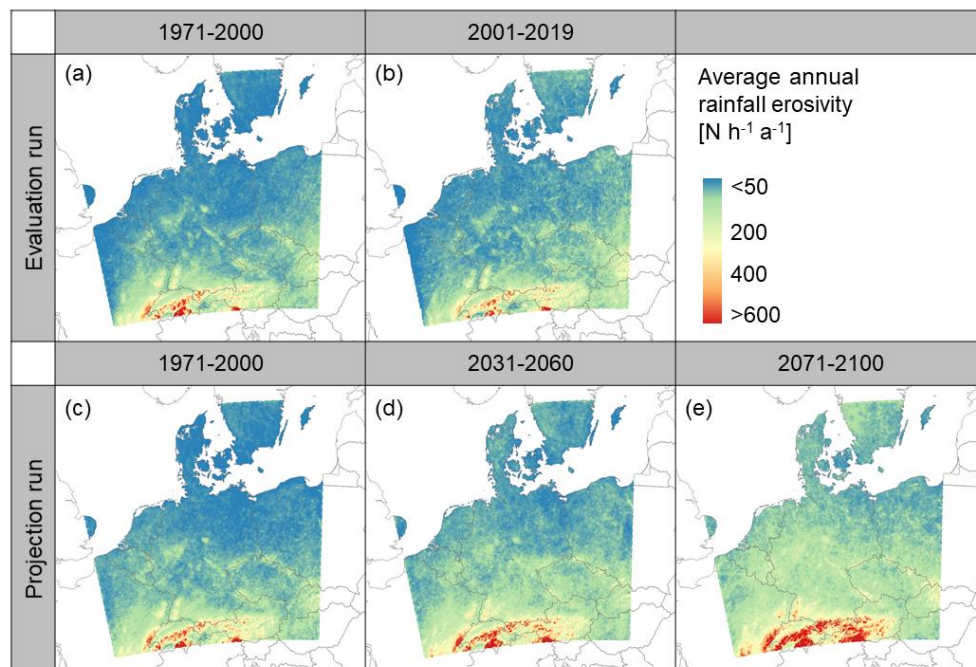
The model was calibrated and validated with average annual suspended sediment loads estimated at 193 measurement sites in the Elbe River basin using a multi-objective optimization technique and stochastic modelling. For further details on the spatial input data, the calibration and the validation of the model, see Uber et al. (2022).

## 250 3 Results and discussions

### 3.1 Past, present and future rainfall erosivity

#### 3.1.1 Rainfall erosivity maps

The average annual rainfall erosivity maps for the five data sets show a consistent spatial pattern (Fig. 2), which is mainly driven by topography. In all datasets erosivity is lowest in the lowlands of the North European Plain and highest in the Alps.  
255 In the past and present, erosivity in the lowlands is on average about  $50 - 90\ N\ h^{-1}\ a^{-1}$ . In the Alps, it ranges on average between 260 and  $290\ N\ h^{-1}\ a^{-1}$  and in the lower mountain ranges it is on average about  $90 - 130\ N\ h^{-1}\ a^{-1}$ . The mean of the entire modeling domain is about  $90 - 96\ N\ h^{-1}\ a^{-1}$ . This value increases to  $119\ N\ h^{-1}\ a^{-1}$  in the near future and  $150\ N\ h^{-1}\ a^{-1}$  in the far future. These maps are available on Zenodo (Uber et al., 2023) and can be used as  $R$ -factor maps in USLE based soil erosion modelling.



260

**Figure 2: Average annual rainfall erosivity (R-factor) in Central Europe in the past, present and future derived from the evaluation run (a-b) and the historic and future projection simulations (c-e).**

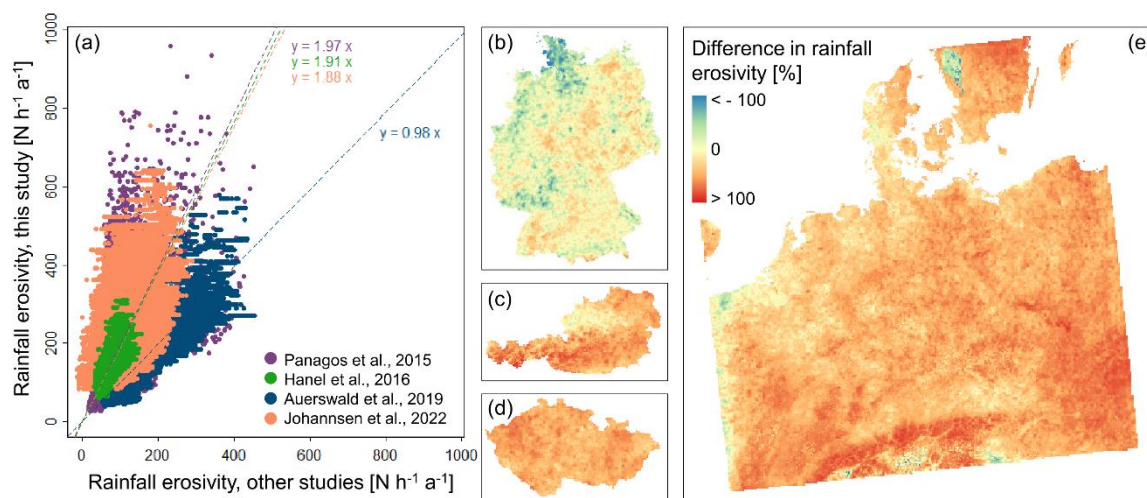
The maps for the past calculated from the evaluation run and the projection run are very similar (Fig. 2a and c). The spatial mean of difference between the maps is  $4.9 \text{ N h}^{-1} \text{ a}^{-1}$  and the values for all grid cells extracted from the two maps correlate well ( $R^2 = 0.91$ , Fig. S1 in the supplementary material).

265

Beyond erosion modelling, rainfall erosivity can also be regarded as an index of heavy rain which combines rainfall intensity and cumulative precipitation depth. As such, it can also provide valuable information for other hydrological applications dealing with extreme rainfalls such as the assessment of (future) risks for flash floods or landslides or identifying zones that are prone to these natural risks (Fiener et al., 2013; Panagos et al., 2015c).



### 270 3.1.2 Comparison to other rainfall erosivity maps



275 **Figure 3: Comparison of the present rainfall erosivity map generated here (evaluation run, data from 2001-2019) with maps presented by other authors. (a) Each point corresponds to a raster cell. The dashed lines show the linear models fit to the data. (b-e) show maps of differences of the map presented here and (b) the map for Germany by Auerswald et al. (2019a) covering the years 2001-2017, (c) the map for Austria covering the years 1995-2015 by Johannsen et al. (2022), (d) for the Czech Republic from 1989-2003 by Hanel et al. (2016b) and (e) for Central Europe covering 1970-2017 with a predominance of the last decade by Panagos et al. (2015c).**

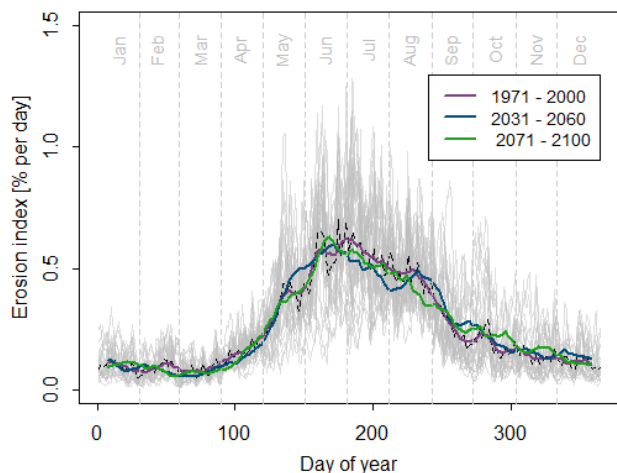
Past and present rainfall erosivity can be compared to other available rainfall erosivity maps. Figure 3 shows that rainfall erosivity calculated from the evaluation simulation for 2001-2019 agrees well with the rainfall erosivity map by Auerswald et al. (2019a). The correlation between the values at the raster cells is very good ( $R^2 = 0.94$ ) and the slope of the linear regression model is 0.98, i.e. very close to one. Thus, there is no systematic difference between the two data sets and the spatial structure corresponds well to the one found by Auerswald et al. (2019a). There are regional differences nonetheless. Rainfall erosivity in the very north of Germany and in the northwest are underestimated here when compared to Auerswald et al. (2019a) and overestimated in parts of eastern Germany, the Black Forest and in the Alps (Fig. 3b). The highest values reported here (>500 N h<sup>-1</sup> a<sup>-1</sup>) are not found by Auerswald et al. (2019a). This might be due to the overestimation of extreme precipitation in COSMO-CLM (Rybka et al., 2022, see Sect. 3.4). Compared to the other rainfall erosivity maps for Europe (Panagos et al., 2015c), the Czech Republic (Hanel et al., 2016b) and Austria (Johannsen et al., 2022), our values are on average about two times higher than the ones of the other authors. Nonetheless, the correlation is good (0.85 – 0.96), so the spatial patterns agree well. In general, differences are highest in the mountains and lower in the plains. Here, we did not correct the precipitation data for snow (i.e. not considering precipitation during days below 0°C) as Johannsen et al. (2022) and Hanel et al. (2016b) did. This can explain parts of the differences, especially in the mountains. The differences can also be due to different temporal coverage of the precipitation data used for the generation of the maps. The temporal coverage of our map (2001-2019) is very similar to the one of the map by Auerswald et al. (2019a) (2001-2017), but agrees less with the temporal coverage of the maps of the other authors (1995-2015 for Johannsen et al. (2022), 1989-2003 for Hanel et al. (2016b) and 1970-2017 with a



295 predominance of the last decade for Panagos et al. (2015c)). Differences in temporal coverage are especially important in the  
presence of trends. Furthermore, our methodology is very similar to the one of Auerswald et al. (2019a) (calculation from  
contiguous data, hourly precipitation data, same temporal scaling factor, same equation used to calculate  $e_{kin,i}$ ) while it differs  
from the methodology used by the other authors.

### 3.1.3 Seasonal distribution of rainfall erosivity

300 The seasonal distribution of rainfall erosivity shows a clear peak in the summer months (late May – August, Fig. 4) and minima  
from November to March. This seasonal pattern is coherent with the results obtained by Johannsen et al. (2022) for Austria,  
by Auerswald et al. (2019a) for Germany and by Meusburger et al. (2012) for Switzerland. There is a strong variability from  
one day to another and between subregions of the modelling domain (light grey lines and dashed black line in Fig. 4). This is  
coherent with the observations made by Auerswald et al. (2019a) and can be explained by the effect of extreme rains that occur  
305 during the same day on several pixels (Auerswald et al., 2019a). Thus, single extreme rainfalls influence the mean values  
despite the large number of pixels and the long averaging period of 30 years.



310 **Figure 4: Seasonal distribution of the erosion index. The light grey lines show daily erosion indexes averaged over 30 years in the  
past (CPS-hist, 1971-2000) and in 25 subregions of the modelling domain. The dashed black line is the average of the entire modeling  
domain in the past and the colored lines show the 13-day moving average for each one of the data sets for the past (CPS-hist, 1971-  
2000), the near future (CPS-scen-nf, 2031-2060) and the far future (CPS-scen-ff, 2071-2100).**

The smoothed distribution of the erosion index does not differ considerably between the past, the near future and the far future  
(Fig. 4). A comparison between past and present rainfall erosivity in Germany by Auerswald et al. (2019b) showed however,  
that winter erosivity increased considerably. In Switzerland on the other hand, Meusburger et al. (2012) observed a decreasing  
315 trend in rainfall erosivity in February despite an increase from May to October. Thus, there might be regions in which seasonal  
shifts occur, but that average out over the larger modelling domain used in this study.



### 3.2 Past and future changes in rainfall erosivity

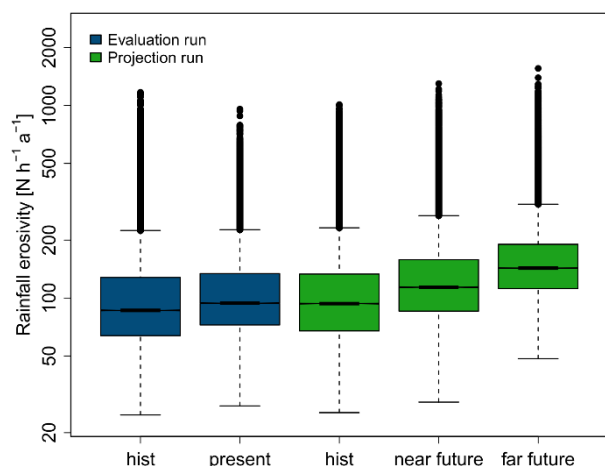


**Figure 5: Distribution of average annual rainfall erosivity (R-factor) [ $\text{N h}^{-1} \text{a}^{-1}$ ] in the five data sets.**

320 In the evaluation run, average annual rainfall erosivity increased between the past (1971-2000, mean:  $90.5 \text{ N h}^{-1} \text{a}^{-1}$ ) and the  
present (2001-2019, mean:  $97.8 \text{ N h}^{-1} \text{a}^{-1}$ ) (Fig. 5). In the projection runs driven by the global climate model, rainfall erosivity  
increased considerably. This is the case for all statistics (Fig. 5). Relative changes in average annual rainfall erosivity (in %)  
between the historical period and the near or far future are highest in the central and northern part of the modeling domain, i.e.  
in the river basins of the Weser, Ems, Elbe and the coastal basins in the north (Fig. 6a and 6b) where rainfall erosivity in the  
325 far future can be up to 84 % higher than in the past. Absolute changes on the other hand are highest in the basins of the Rhine  
( $28 \text{ N h}^{-1} \text{a}^{-1}$  in the near future and  $78 \text{ N h}^{-1} \text{a}^{-1}$  in the far future) and the Upper Danube ( $37$  and  $74 \text{ N h}^{-1} \text{a}^{-1}$  respectively). These  
are very strong changes that lead to a strong increase in future soil erosion rates (Sect. 3.3). Furthermore, the changes in rainfall  
erosivity calculated from convection-permitting climate model output are considerably higher than the ones calculated with  
the low-resolution approach using mean annual precipitation from model output of conventional regional climate model  
330 ensembles (Fig. 6c and 6d).

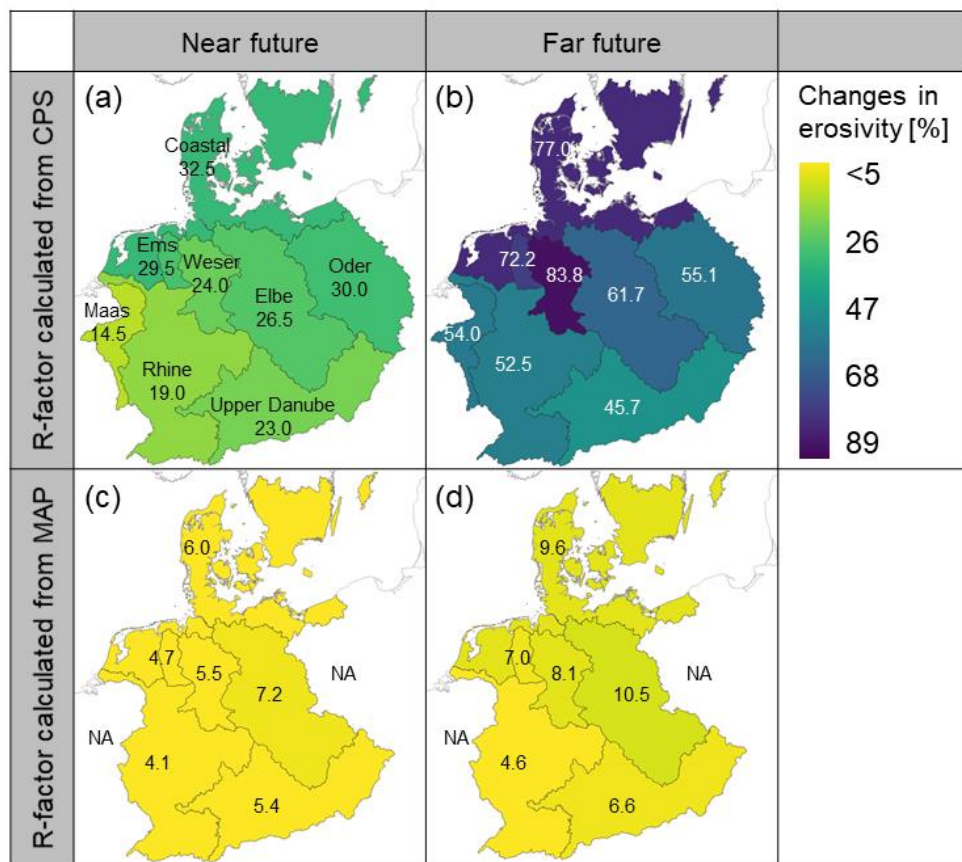


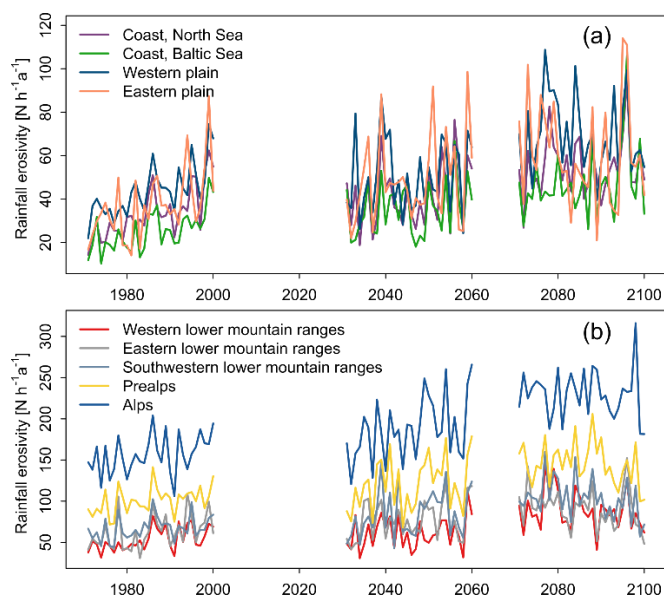
Figure 6: Relative changes in average annual rainfall erosivity (R-factor) in the major Central European river basins between the historical period (1971-2000) and the near future (2031-2060, (a) and (c)) or the far future (2071-2100, (b) and (d)). All values are given in percent of the erosivity of the historical period. The top row shows changes in erosivity calculated with the convection-permitting simulations (CPS); the bottom row shows changes in erosivity calculated with mean annual precipitation (MAP) obtained from the median of 21 regional climate models. All simulations used emission scenario RCP 8.5.

This finding is in line with the results of Gericke et al. (2019) who also note that the low-resolution approach underestimates rainfall erosivity and future changes in erosivity. The regression equation of the German DIN 19708 that was used here (Eq. 3) was established in the early 1990s with climate data from the 1960s to 1980s. Thus, its age and the fact that it does not consider heavy precipitation raise concerns that the equation can be transferred to the future (Gericke et al., 2019). It has to be noted that DIN 19708 explicitly states that whenever possible, high frequency precipitation should be used and that using Eq. (3) should only be used when only monthly or annual precipitation is available.

Annual rainfall erosivity in all topographic regions of Central Europe (coasts, plains, low mountain ranges, Prealps and Alps) shows a strong interannual variability and clear trends (Fig. 7). The high interannual variability observed here is consistent with the findings of other authors who observed strong interannual variability in rainfall erosivity calculated from measured precipitation data (e.g. Verstraeten et al., 2006; Meusburger et al., 2012; Fiener et al., 2013). The presence of trends supports



the conclusions made by other authors that rainfall erosivity maps have to be frequently updated because old rainfall erosivity maps no longer represent current precipitation characteristics (Auerswald et al., 2019b; Johannsen et al., 2022).



350 **Figure 7: Trends and interannual variability in rainfall erosivity in the natural regions of Central Europe (coast and plains (a) as well as lower mountain ranges, Prealps and Alps (b)). Rainfall erosivity was calculated with precipitation data from the projection run. The natural regions were defined according to Bundesamt für Naturschutz (2017) for Germany and were manually extended to include Central Europe based on elevation here. They are outlined in Fig. 1.**

While calculating future rainfall erosivity from CPS offers the advantage of the direct calculation from high-resolution data, it only represents future projections from one model and one emission scenario which is less robust than using model ensembles. Thus, we compared the past and future changes calculated here to observed and simulated trends in rainfall erosivity in central Europe reported in the literature (Table S1, supplementary material). Both in the past and in the future, the range of reported trends is very large. The values given here agree well with reported values in some cases (e.g. approx. 20 % increase per decade in the Ruhr area in Germany calculated here for the projection run and reported by Fiener et al. (2013) in the period 1973-2007). In other cases, they are strongly over- or underestimated (Table S1). It also has to be noted that for the period 1971-2000 where we estimated rainfall erosivity from the projection run as well as from the evaluation run, the trends in the two data sets can differ considerably. Usually, the changes were stronger in the projection run than in the evaluation run.

The high range of trends reported in the literature shows the need to consider model ensembles and to conduct sensitivity analyses to differences in methodology in future research. Even though the changes calculated here from CPS are considerably higher than the ones estimated previously with a low-resolution approach and conventional regional climate model output, a comparison with the literature suggests that actual future changes could even be higher than reported here. Such strong changes in rainfall erosivity in the order of > 10 % per decade would have important implication for future soil erosion as well as for the occurrence of other natural risks such as landslides and flash floods that are triggered by heavy rain events.



### 3.3 Simulated soil erosion rates in the Elbe River basin

370 In the Elbe River basin, soil erosion rates are highest on rolling arable land in the central part of the catchment as well as in  
 the Czech part of the basin. This spatial pattern is found in both sets of simulations (R-factor calculated with data from mean  
 annual precipitation (MAP) or CPS) (Fig. 8). The order of magnitude of erosion rates is also the same, because both realizations  
 of the soil erosion model are calibrated with the same data set of measured sediment loads. However, as rainfall erosivity  
 calculated from CPS is considerably higher than the one calculated from MAP, the optimized values for the transport capacity  
 375 coefficient are approx. two times higher when rainfall erosivity was calculated from MAP compared to calculations from CPS.

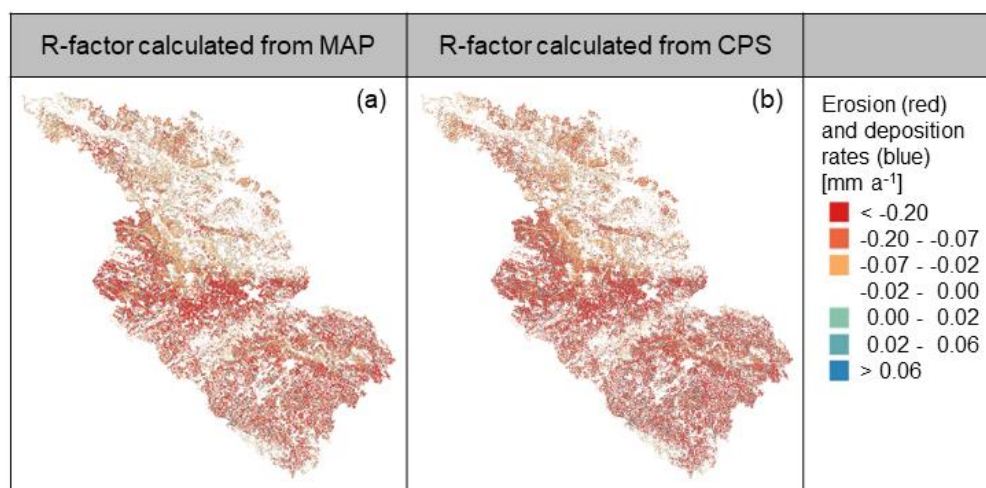
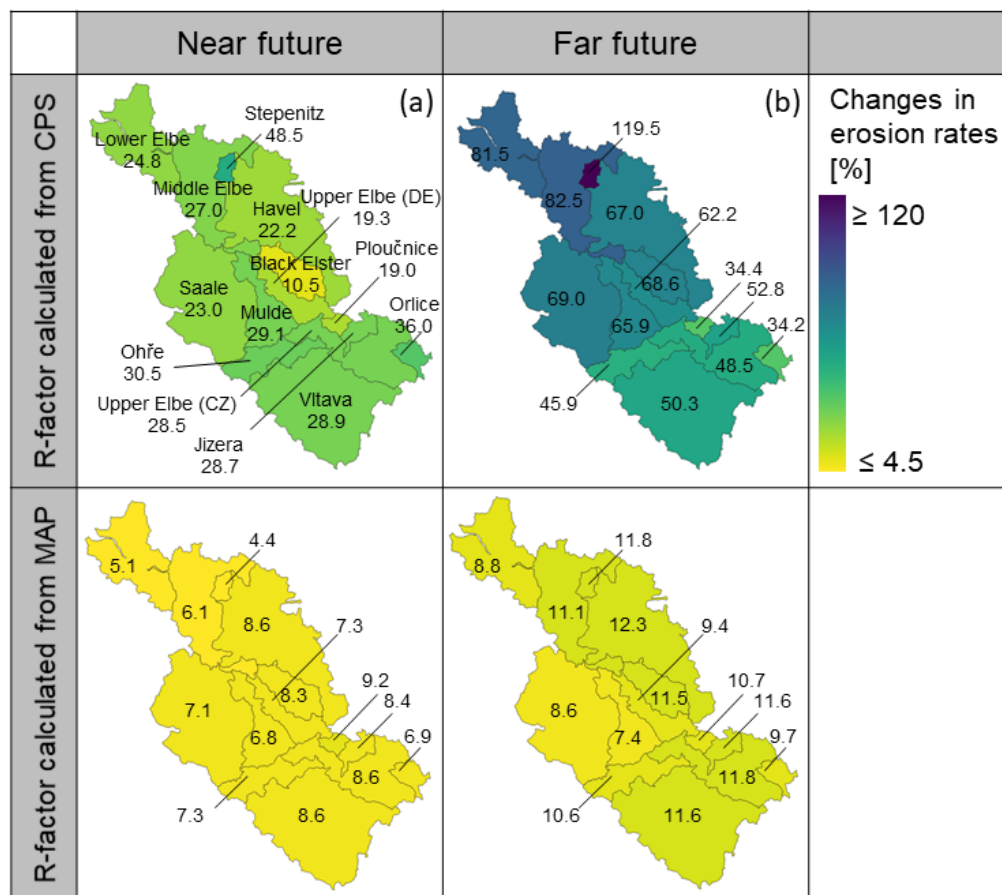


**Figure 8:** Past (1971-2000) erosion and deposition rates in the Elbe River basin simulated with WaTEM/SEDEM and R-factors calculated from mean annual precipitation (a) or convection-permitting simulations (b).

The future projections of soil erosion rates, on the other hand, differ a lot between the two model realizations. When future  
 380 erosivity is calculated from MAP obtained from the median of 21 climate models in the DWD reference ensemble run with  
 the emission scenario RCP 8.5, erosion rates increase by 4.4 – 9.2 % in the subbasins of the Elbe River basin in the near future  
 and by 7.4 – 12.3 % in the far future (Fig. 9c and d). These values are considerably higher when future erosivity is calculated  
 from CPS (10.5 – 48.5 % in the near future and 34.2 – 119.5 % in the far future, Fig. 9a and b). The changes (in percent of  
 historic erosion rates) are highest in the northern part of the basin where erosion rates are low due to the flat terrain. But also  
 385 in the subbasins of the Saale, Mulde and German Upper Elbe where erosion rates are high, erosion rates are projected to change  
 by 19.3 – 29.1 % in the near future and 62.2 - 69.0 % in the far future. In these subbasins, absolute changes are highest.





390 **Figure 9: Simulated relative changes in soil erosion rates in the subbasins of the Elbe River basin between the historical period (1971-2000) and the near future (2031-2060, (a) and (c)) or the far future (2071-2100, (b) and (d)). Rainfall erosivity is either calculated from convection-permitting simulations (CPS, (a) and (b)) or from mean annual precipitation (MAP, (c) and (d)).**

The changes in erosion rates lead to changes in sediment delivery to water bodies that are similar to or slightly higher than the change rates shown in Fig. 9. For example, at the outlet of the Vltava, sediment loads increase on average by 35.5 % in the near future and by 57.5 % in the far future and at the outlet of the Saale by 21.4 % and 70.7 % respectively. At the most downstream measurement station of the Elbe at Hitzacker, sediment loads increase by 22.9 % and 69.0 % respectively. It has to be noted that the reported changes are the result of changes in rainfall erosivity alone while changes in sediment connectivity, land cover and management are not considered here.

Our results show that USLE-based simulations of future changes in soil erosion are highly sensitive to the calculation of future R-factors. A similar observation was made by Eekhout and De Vente (2020) who assessed how soil erosion conceptualizations affect soil loss projections under climate change. They compared a RUSLE-based model forced by monthly precipitation, a model based on the Modified Universal Soil Loss Equation (MUSLE, Williams and Berndt, 1977; Williams, 1995) forced by runoff and the MMF model (Morgan et al., 1984; Morgan and Duzant, 2008) forced by both precipitation and runoff. They



also found that the RUSLE-based model forced with monthly precipitation cannot represent changes in extreme precipitation. Thus, in their Mediterranean study site, the RUSLE-based model projected a decrease in soil loss while the other two models projected an increase. Here, we argue that this underestimation of future soil loss with respect to the other models is not  
405 inherent in the RUSLE but caused by the low-resolution approach of calculating rainfall erosivity. Nonetheless, it is very important to compare different model conceptualizations and to include runoff as a driver of soil erosion. Here, the use of the high spatio-temporal resolution model output of convection-permitting climate models also has a high potential for future research using coupled hydrological and soil erosion models that can include runoff as a driver of soil erosion.

### 3.4 Potential and limitations of convection-permitting climate simulations for the calculation of rainfall erosivity

410 The maps presented here offer a high potential for erosion modelling and climate impact studies. Due to the high resolution of 3 km, they can represent the high spatial variability of rainfall erosivity in a large domain in Central Europe. Unlike most other R-factor maps (Meusburger et al., 2012; Panagos et al., 2015c; Hanel et al., 2016b), our maps do not rely on spatial interpolation and correlation with other spatial covariates such as elevation, latitude, longitude or climate indices.

Because of the high temporal resolution of the underlying precipitation data, we did not have to rely on correlations between  
415 R-factors calculated at a high resolution and low-resolution rainfall totals such as MAP, either. Many studies find a good correlation between MAP and R-factors, suggesting that MAP is a good covariate to estimate R at locations where no high-resolution precipitation data is available. However, using empirical relations between past MAP and past R-factors to derive future R-factors is problematic because it is unlikely that these relations remain stationary in the future (Quine and Van Oost, 2020). These relations are strongly conditioned by the frequency and magnitude of rainfall events that will very likely change  
420 in a warmer climate. In several regions in Europe such as the Mediterranean (Tramblay, 2012; Blanchet, 2018) and the Carpathian Basin (Bartholy and Pongrácz, 2007), MAP is decreasing while extreme precipitation is increasing. This leads to an underestimation of future R-factors that are derived from MAP alone. In Central Europe, both MAP and extreme precipitation are expected to increase (Jacob et al., 2014; Brienens et al., 2020), so future R-factors derived from MAP are also underestimated but less severely than in the above-mentioned regions. Because changes in MAP as well as in extreme  
425 precipitation are well represented in convection-permitting simulations, they offer a valuable data source for the calculation of future rainfall erosivity.

Even when the same temporal resolution of simulated precipitation data is used, Chapman et al. (2021) find that rainfall erosivity was considerably higher and observed storm characteristics agreed better with simulated ones when a convection-permitting model was used instead of a conventional convection-parameterized one.

430 On the other hand, the maps presented here also have limitations. Here, we calculated rainfall erosivity from precipitation data and did not consider whether precipitation falls as rain, snow or hail, so the high erosivity of hail is underestimated while erosivity in zones where considerable amounts of precipitation fall as snow (i.e. mainly the Alps) is overestimated. As rainfall erosivity in Central Europe is highest in the summer month, we assume that the impact of snow is small and can be neglected. For the Alps this is not the case, thus the very high values calculated in this region are too high. A further limitation inherent



435 in the USLE is that erosivity is calculated from rainfall data alone even though runoff rate is the driving force of soil detachment  
and transport once rills are activated (Nearing et al., 2017). Runoff-driven entrainment of soil particles is considered in the  
MUSLE and other models such as WEPP (Laflen, 1991), LISEM (De Roo et al., 1996), MMF (Morgan and Duzant, 2008),  
PESERA (Kirkby, 2008) or the ones presented by Cea et al. (2016), Nord and Esteves (2005) and Favis-Mortlock et al. (2000),  
but these require more complex hydrological and hydraulic modelling, which limits their applicability in the context of larger  
440 river systems.

As our maps are calculated from model output and not from precipitation measurements, the uncertainties of the model are  
propagated to the rainfall erosivity maps. The precipitation data was quality controlled and compared to radar- and station-  
based precipitation data from the past but not bias-corrected. The data showed a good agreement for extreme rainfall intensities  
for durations of more than 12 h but an overestimation for hourly extreme precipitation intensities (Rybka et al., 2022). Thus,  
445 it is important to compare the R-factors calculated here to the ones calculated from measured rainfall data.

Concerning the future projections, it has to be noted that current climate models struggle with estimates of future precipitation  
and biases are much larger than those for future temperatures (e.g. Slingo et al., 2022). Ensembles of global and regional  
climate models show a high range of future trends in precipitation that cannot be represented by a single model. Other studies  
estimated future R-factors from ensembles of global or regional climate models such as the CMIP5 model ensemble, the  
450 EURO-CORDEX ensemble or the DWD reference ensemble (Gericke et al., 2019; Panagos et al., 2022; Uber et al., 2022). In  
this way, the high range in projections can be represented and the uncertainty due to the choice of climate model and emission  
scenario can be assessed. To date, this is not possible for convection-permitting climate models because there are no model  
ensembles of multi-decadal simulations over large domains yet available. However, there are promising flagship studies such  
as the CORDEX-FPS where a first multi-model convection-permitting ensemble for the Alps and the Mediterranean is  
455 presented (Coppola et al., 2020). Thus, the soil erosion modelling community should follow closely the coming advances in  
convection-permitting modelling to take advantage of new climate simulations for climate impact studies.

#### 4 Conclusions

We calculated rainfall erosivity (quantified as the USLE R-factor) in Central Europe in the past (1971-2000), present (2001-  
2019), near future (2031-2060) and far future (2071-2100) from convection-permitting climate simulation (CPS) output. From  
460 this work, we draw three main conclusions:

- Thanks to the high spatio-temporal resolution of CPS (in this case 3 km, 1 h), R-factors can be calculated directly  
without having to rely on spatial interpolation and regression with aggregated precipitation sums such as mean annual  
precipitation (MAP). Thus, CPS offer a high potential for the calculation of future R-factors for climate impact studies  
on soil erosion. For the present, the R-factor map presented here is very similar to the map by Auerswald et al. (2019)  
465 that was calculated from radar-derived precipitation data.



- 470 • In the river basins in Central Europe, changes in rainfall erosivity between the past and the near future can be as high as 33 % and in the far future it can be up to 84 % higher. In the Elbe River basin, this leads to much higher rates of soil erosion (locally up to 120 % increase). These rates of change are much higher than estimated previously using regression with MAP (up to 7 % higher rainfall erosivity in the near future, 10 % in the far future). This is due to the fact that the intensification of extreme precipitation is not represented by changes in MAP. This indicates that correlations between R-factors and MAP that were developed in the past are not necessarily valid in the future.
- 475 • A major limitation of CPS is their high computational demand. Thus, model domains are usually limited to much smaller spatial extents than the ones covered by global or regional climate models or simulated time periods are limited to short time periods. The simulations in COSMO CLM cover a long time period (in total 109 years) and a comparably large modeling domain of approx. 1.6 million km<sup>2</sup> on land. However, to date no ensembles of CPS are available at the regional scale and for long time periods. Thus, in contrast to global or regional climate models, the uncertainty in future R-factors due to the choice of climate models cannot yet be estimated by using a bandwidth of model ensembles. Promising advances in the CPS community – including flagship studies on CPS model ensembles – suggest that in the future more CPS will be available for climate impact studies on soil erosion.

#### 480 **Data Availability**

COSMO-CLM model output (e.g. hourly precipitation) is freely available from the evaluation simulations CPS-eval (Brienen et al., 2022), the historical projection simulations CPS-hist (Haller et al., 2022a) and the scenario projection simulations CPS-scen (Haller et al., 2022b) at <https://esgf.dwd.de/projects/dwd-cps/> (accessed 10 February 2023). The rainfall erosivity maps presented in Fig. 2 are available at <https://doi.org/10.5281/zenodo.7628957> (accessed 20 march 2023, Uber et al., 2023).

#### 485 **Author contribution**

MU and GH conceived and designed the study with contributions by all coauthors. MU performed the analyses and calculations with contributions by TH, CB and MH. MH performed simulations with COSMO-CLM and provided data. MU wrote the original draft with contributions by MH. MU created the figures. GH, TH and CB reviewed and edited the draft. GH acquired funding and was responsible for project administration.

#### 490 **Competing interests**

The authors declare that they have no conflict of interest.



## Acknowledgements

This research was funded by the German Federal Ministry for Digital and Transport Network of Experts. We want to thank our colleagues at the Federal Institute of Hydrology (BfG) and DWD as well as the members of the Network of Experts  
495 Themenfeld 1 for the fruitful discussions. R-factor calculations were run at the BfG's high-performance computers. We thank the maintainers and users for the provision of the infrastructure and useful advices. The COSMO-CLM is a regional climate model maintained by the CLM-Community. We thank the community members for their support.

## References

- Alexander, L. V., Zhang, X., Peterson, T. C., Caesar, J., Gleason, B., Klein Tank, A., Haylock, M., Collins, D., Trewin, B.,  
500 Rahimzadeh, F., Tagipour, A., Rupa Kumar, K., Revadekar, J., Griffiths, G., Vincent, L., Stephenson, D. B., Burn, J., Aguilar, E., Brunet, M., Taylor, M., New, M., Zhai, P., Rusticucci, M., and Vazquez-Aguirre, J. L.: Global observed changes in daily climate extremes of temperature and precipitation, *J GEOPHYS RES-ATMOS*, 111, D05109, <https://doi.org/10.1029/2005JD006290>, 2006.
- Allen, M. R. and Ingram, W. J.: Constraints on future changes in climate and the hydrologic cycle, *NATURE*, 419, 224-232,  
505 <https://doi.org/10.1038/nature01092>, 2002.
- Amundson, R., Berhe, A. A., Hopmans, J. W., Olson, C., Sztein, A. E., and Sparks, D. L.: Soil and human security in the 21st century, *SCIENCE*, 348, 1261071, <https://doi.org/10.1126/science.1261071>, 2015.
- Arnold, J. G., Srinivasan, R., Muttiah, R. S., and Williams, J. R.: Large area hydrologic modeling and assessment part I: model development 1, *J AM WATER RESOUR AS*, 34, 73-89, <https://doi.org/10.1111/j.1752-1688.1998.tb05961.x>, 1998.
- 510 Arnone, E., Pumo, D., Viola, F., Noto, L. V., and La Loggia, G.: Rainfall statistics changes in Sicily, *HYDROL EARTH SYST SC*, 17, 2449-2458, <https://doi.org/10.5194/hess-17-2449-2013>, 2013.
- Auerswald, K., Fischer, F., Winterrath, T., and Brandhuber, R.: Rain erosivity map for Germany derived from contiguous radar rain data, *HYDROL EARTH SYST SC*, 23, 1819-1832, <https://doi.org/10.5194/hess-23-1819-2019>, 2019a.
- Auerswald, K., Fischer, F., Winterrath, T., Elhaus, D., Maier, H., and Brandhuber, R.: Klimabedingte Veränderung der  
515 Regenerosivität seit 1960 und Konsequenzen für Bodenabtragsschätzungen, in: *Bodenschutz, Ergänzbare Handbuch der Maßnahmen und Empfehlungen für Schutz, Pflege und Sanierung von Böden, Landschaft und Grundwasser*, edited by: Bachmann G., König W., Utermann J., Erich Schmidt Verlag, Berlin, Germany, 21 pp., 2019b.
- Ban, N., Schmidli, J., and Schär, C.: Evaluation of the convection-resolving regional climate modeling approach in decade-long simulations, *J GEOPHYS RES-ATMOS*, 119, 7889-7907, <https://doi.org/10.1002/2014JD021478>, 2014.
- 520 Ban, N., Cécile, C., Coppola, E., Pichelli, E., Sobolowski, S., Adinolfi, M., Ahrens, B., Alias, A., Anders, I., Bastin, S., Belušić, D., Berthou, S., Brisson, E., Cardoso, R. M., Chan, S. C., Christensen, O. B., Fernández, J., Fita, L., Frisius, T., Gašparac, G., Giorgi, F., Goergen, K., Haugen, J. E., Hodnebrog, Ø., Kartsios, S., Katragkou, E., Kendon, E. J., Keuler, K., Lavin-Gullon, A., Lenderink, G., Leutwyler, D., Lorenz, T., Maraun, D., Mercogliano, P., Milovac, J., Panitz, H.-J., Raffa, M., Remedio, A.



- R., Schär, C., Soares, P. M. M., Srnec, L., Steensen, B. M., Stocchi, P., Tölle, M. H., Truhetz, H., Vergara-Temprado, J., de  
525 Vries, H., Warrach-Sagi, K., Wulfmeyer, V., and Zander, M. J.: The first multi-model ensemble of regional climate simulations  
at kilometer-scale resolution, part I: evaluation of precipitation, *CLIM DYNAM*, 57, 275-302, <https://doi.org/10.1007/s00382-021-05708-w>, 2021.
- Bartholy, J. and Pongrácz, R.: Regional analysis of extreme temperature and precipitation indices for the Carpathian Basin  
from 1946 to 2001, *GLOBAL PLANET CHANGE*, 57, 83-95, <https://doi.org/10.1016/j.gloplacha.2006.11.002>, 2007.
- 530 Berg, P., Moseley, C., and Haerter, J. O.: Strong increase in convective precipitation in response to higher temperatures, *NAT  
GEOSCI*, 6, 181-185, <https://doi.org/10.1038/ngeo1731>, 2013.
- Bergemann, M., Blöcker, G., Harms, H., Kerner, M., Meyer-Nehls, R., Petersen, W., and Schroeder, F.: Der Sauerstoffhaushalt  
der Tidelbe, *Die Küste*, 58, 199-261, 1996.
- Bilotta, G. S. and Brazier, R. E.: Understanding the influence of suspended solids on water quality and aquatic biota, *WATER  
535 RES*, 42, 2849-2861, <https://doi.org/10.1016/j.watres.2008.03.018>, 2008.
- Blanchet, J., Moliné, G., and Touati, J.: Spatial analysis of trend in extreme daily rainfall in southern France, *CLIM DYNAM*,  
51, 799-812, 2018.
- Böhm, U., Kücken, M., Ahrens, W., Block, A., Hauffe, D., Keuler, K., Rockel, B., and Will, A.: CLM-the climate version of  
LM: brief description and long-term applications. *COSMO newsletter*, 6, 225 - 235, 2006.
- 540 Borrelli, P., Robinson, D. A., Panagos, P., Lugato, E., Yang, J. E., Alewell, C., Wuepper, D., Montanarella, L., and Ballabio,  
C.: Land use and climate change impacts on global soil erosion by water (2015-2070), *Proceedings of the National Academy  
of Sciences*, 117, 21994-22001, <https://doi.org/10.1073/pnas.2001403117>, 2020.
- Borrelli, P., Christine, A., Pablo, A., Ayach, A. J. A., Jantiene, B., Cristiano, B., Nejc, B., Marcella, B., Cerda, A., Chalise, D.,  
and others: Soil erosion modelling: A global review and statistical analysis, *SCI TOTAL ENVIRON*, 780, 146494,  
545 <https://doi.org/10.1016/j.scitotenv.2021.146494>, 2021.
- Brienen, S., Water, A., Brendel, C., Fleischer, C., Ganske, A., Haller, M., Helms, M., Höpp, S., Jensen, C., Jochumsen, K.,  
Möller, J., Krähenmann, S., Nilson, E., Rauthe, M., Razafimaharo, C., Rudolph, E., Rybka, H., Schade, N., and Stanley, K.:  
Klimawandelbedingten Änderungen in Atmosphäre und Hydrosphäre. Schlussbericht des Schwerpunktthemas  
Szenarienbildung (SP-101) im Themenfeld 1 des BMVI-Expertennetzwerk, 157 pp.,  
550 <https://doi.org/10.5675/ExpNBS2020.2020.02>, 2020.
- Brienen, S., Haller, M., Brauch, J., and Früh, B.: HoKliSim-De evaluation simulation with COSMO-CLM5-0-16 version  
V2022.01 [dataset], [https://doi.org/10.5676/DWD/HOKLISIM\\_V2022.01](https://doi.org/10.5676/DWD/HOKLISIM_V2022.01), 2022.
- Brychta, J., Podhrázká, J., and Šťastná, M.: Review of methods of spatio-temporal evaluation of rainfall erosivity and their  
correct application, *CATENA*, 217, 106454, <https://doi.org/10.1016/j.catena.2022.106454>, 2022.
- 555 Bundesamt für Naturschutz: Naturräume und Großlandschaften Deutschlands (n.Ssymank) [dataset], 2017.



- Cea, L., Legout, C., Grangeon, T., and Nord, G.: Impact of model simplifications on soil erosion predictions: application of the GLUE methodology to a distributed event-based model at the hillslope scale, *HYDROL PROCESS*, 30, 1096-1113, <https://doi.org/10.1002/hyp.10697>, 2016.
- Chapman, S., Birch, C. E., Galdos, M. V., Pope, E., Davie, J., Bradshaw, C., Eze, S., and Marsham, J. H.: Assessing the impact of climate change on soil erosion in East Africa using a convection-permitting climate model, *ENVIRON RES LETT*, 16, 084006, <https://doi.org/10.1088/1748-9326/ac10e1>, 2021.
- Ciszewski, D. and Grygar, T. M.: A review of flood-related storage and remobilization of heavy metal pollutants in river systems, *WATER AIR SOIL POLL*, 227, 239, <https://doi.org/10.1007/s11270-016-2934-8>, 2016.
- Copernicus Land Monitoring Service: European Digital Elevation Model (EU-DEM), version 1.1 (1.1) [dataset], 2016.
- 565 Copernicus Land Monitoring Service: Corine Land Cover (CLC) 1990, version 2020\_20u1 [dataset], 2019.
- Coppola, E., Sobolowski, S., Pichelli, E., Raffaele, F., Ahrens, B., Anders, I., Ban, N., Bastin, S., Belda, M., Belusic, D., Caldas-Alvarez, A., Cardoso, R. M., Davolio, S., Dobler, A., Fernandez, J., Fita, L., Fumiere, Q., Giorgi, F., Goergen, K., Güttler, I., Halenka, T., Heinzeller, D., Hodnebrog, Ø., Jacob, D., Kartsios, S., Katragkou, E., Kendon, E., Khodayar, S., Kunstmann, H., Knist, S., Lavín-Gullón, A., Lind, P., Lorenz, T., Maraun, D., Marelle, L., van Meijgaard, E., Milovac, J., 570 Myhre, G., Panitz, H. J., Piazza, M., Raffa, M., Raub, T., Rockel, B., Schär, C., Sieck, K., Soares, P. M. M., Somot, S., Srnec, L., Stocchi, P., Tölle, M. H., Truhetz, H., Vautard, R., de Vries, H., and Warrach-Sagi, K.: A first-of-its-kind multi-model convection permitting ensemble for investigating convective phenomena over Europe and the Mediterranean, *CLIM DYNAM*, 55, 3-34, <https://doi.org/10.1007/s00382-018-4521-8>, 2020.
- Coulthard, T. J., Ramirez, J., Fowler, H. J., and Glenis, V.: Using the UKCP09 probabilistic scenarios to model the amplified 575 impact of climate change on drainage basin sediment yield, *HYDROL EARTH SYST SC*, 16, 4401-4416, <https://doi.org/10.5194/hess-16-4401-2012>, 2012.
- De Roo, A., Offermans, R., and Cremers, N.: LISEM: A single-event, physically based hydrological and soil erosion model for drainage basins. II: Sensitivity analysis, validation and application, *HYDROL PROCESS*, 10, 1119-1126, [https://doi.org/10.1002/\(SICI\)1099-1085\(199608\)10:8<1119::AID-HYP416>3.0.CO;2-V](https://doi.org/10.1002/(SICI)1099-1085(199608)10:8<1119::AID-HYP416>3.0.CO;2-V), 1996.
- 580 DIN-Normenausschuss Wasserwesen: DIN 19708:2017-08 Bodenbeschaffenheit - Ermittlung der Erosionsgefährdung von Böden durch Wasser mit Hilfe der ABAG, <https://doi.org/10.31030/2676773>, 2017.
- Doms, G., Förstner, J., Heise, E., Herzog, H., Mironov, D., Raschendorfer, M., Reinhardt, T., Ritter, B., Schrodin, R., and Schulz, J.-P.: A description of the nonhydrostatic regional COSMO model, Part II: Physical Parameterization, *Deutscher Wetterdienst*, Offenbach, Germany, 177 pp., 2011.
- 585 Eekhout, J. P. C. and De Vente, J.: How soil erosion model conceptualization affects soil loss projections under climate change, *Progress in Physical Geography: Earth and Environment*, 44, 212-232, <https://doi.org/10.1177/0309133319871937>, 2020.
- Favis-Mortlock, D. T., Boardman, J., Parsons, A. J., and Lascelles, B.: Emergence and erosion: a model for rill initiation and development, *HYDROL PROCESS*, 14, 2173-2205, [https://doi.org/10.1002/1099-1085\(20000815/30\)14:11/12<2173::AID-HYP61>3.0.CO;2-6](https://doi.org/10.1002/1099-1085(20000815/30)14:11/12<2173::AID-HYP61>3.0.CO;2-6), 2000.



- 590 Fiener, P., Neuhaus, P., and Botschek, J.: Long-term trends in rainfall erosivity—analysis of high resolution precipitation time series (1937–2007) from Western Germany, *AGR FOREST METEOROL*, 171, 115–123, <https://doi.org/10.1016/j.agrformet.2012.11.011>, 2013.
- Fischer, E. M. and Knutti, R.: Observed heavy precipitation increase confirms theory and early models, *NAT CLIM CHANGE*, 6, 986–991, <https://doi.org/10.1038/nclimate3110>, 2016.
- 595 Fischer, F. K., Winterrath, T., and Auerswald, K.: Temporal- and spatial-scale and positional effects on rain erosivity derived from point-scale and contiguous rain data, *HYDROL EARTH SYST SC*, 22, 6505–6518, <https://doi.org/10.5194/hess-22-6505-2018>, 2018.
- Fowler, H. J., Lenderink, G., Prein, A. F., Westra, S., Allan, R. P., Ban, N., Barbero, R., Berg, P., Blenkinsop, S., Do, H. X., and et al.: Anthropogenic intensification of short-duration rainfall extremes, *NAT REV EARTH ENVIRON*, 2, 107–122, <https://doi.org/10.1038/s43017-020-00128-6>, 2021.
- 600 Gericke, A., Kiesel, J., Deumlich, D., and Venohr, M.: Recent and future changes in rainfall erosivity and implications for the soil erosion risk in Brandenburg, NE Germany, *WATER-SUI*, 11, 904, <https://doi.org/10.3390/w11050904>, 2019.
- Giorgetta, M., Brokopf, R., Crueger, T., Esch, M., Fiedler, S., Helmert, J., Hohenegger, C., Kornblueh, L., Köhler, M., Manzini, E., Mauritsen, T., Nam, C., Raddatz, T., Rast, S., Reinert, D., Sakradzija, M., Schmidt, H., Schneck, R., Schnur, R.,
- 605 Silvers, L., Wan, H., Zängl, G., and Stevens, B.: ICON-A, the Atmosphere Component of the ICON Earth System Model: I. Model Description, *J ADV MODEL EARTH SY*, 10, 1613–1637, <https://doi.org/10.1029/2017MS001242>, 2018.
- Groisman, P. Y., Knight, R. W., Easterling, D. R., Karl, T. R., Hegerl, G. C., and Razuvaev, V. N.: Trends in intense precipitation in the climate record, *J CLIMATE*, 18, 1326–1350, <https://doi.org/10.1175/JCLI3339.1>, 2005.
- Haller, M., Brienens, S., Brauch, J., and Früh, B.: Historical simulation with COSMO-CLM5-0-16, version V2022.01 [dataset], [https://doi.org/10.5676/DWD/CPS\\_HIST\\_V2022.01](https://doi.org/10.5676/DWD/CPS_HIST_V2022.01), 2022a.
- 610 Haller, M., Brienens, S., Brauch, J., and Früh, B.: Projection simulation with COSMO-CLM5-0-16, version V2022.01 [dataset], [https://doi.org/10.5676/DWD/CPS\\_SCEN\\_V2022.01](https://doi.org/10.5676/DWD/CPS_SCEN_V2022.01), 2022b.
- Haller, M., Brienens, S., Rybka, H., Winterrath, T., Kunert, L., and Früh, B.: Convection-permitting climate simulations with COSMO-CLM: Evaluation of heavy rain fall for Germany, *METEOROL Z*, 2023, in preparation.
- 615 Hanel, M., Pavlásková, A., and Kyselý, J.: Trends in characteristics of sub-daily heavy precipitation and rainfall erosivity in the Czech Republic, *INT J CLIMATOL*, 36, 1833–1845, <https://doi.org/10.1002/joc.4463>, 2016a.
- Hanel, M., Máca, P., Bašta, P., Vlnas, R., and Pech, P.: The rainfall erosivity factor in the Czech Republic and its uncertainty, *HYDROL EARTH SYST SC*, 20, 4307–4322, <https://doi.org/10.5194/hess-20-4307-2016>, 2016b.
- Hersbach, H., Bell, B., Berrisford, P., Hirahara, S., Horányi, A., Muñoz-Sabater, J., Nicolas, J., Peubey, C., Radu, R., Schepers, D., Simmons, A., Soci, C., Abdalla, S., Abellan, X., Balsamo, G., Bechtold, P., Biavati, G., Bidlot, J., Bonavita, M., De Chiara, G., Dahlgren, P., Dee, D., Diamantakis, M., Dragani, R., Flemming, J., Forbes, R., Fuentes, M., Geer, A., Haimberger, L., Healy, S., Hogan, R. J., Hólm, E., Janisková, M., Keeley, S., Laloyaux, P., Lopez, P., Lupu, C., Radnoti, G., de Rosnay, P.,





- Rozum, I., Vamborg, F., Villaume, S., and Thépaut, J.-N.: The ERA5 global reanalysis, *Q J ROY METEOR SOC*, 146, 1999-2049, <https://doi.org/10.1002/qj.3803>, 2020.
- 625 ICPER (International Commission for the Protection of the Elbe River): Sedimentmanagementkonzept der IKSE-Vorschläge für eine gute Sedimentmanagementpraxis im Elbegebiet zur Erreichung überregionaler Handlungsziele, ICPER, Magdeburg, Germany, 202 pp., 2014.
- ICPER (International Commission for the Protection of the Elbe River): The Elbe River and its Basin, ICPER, Magdeburg, Germany, 2 pp., 2016.
- 630 Jacob, D., Petersen, J., Eggert, B., Alias, A., Christensen, O. B., Bouwer, L. M., Braun, A., Colette, A., Déque, M., Georgievski, G., Georgopoulou, E., Gobiet, A., Menut, L., Nikulin, G., Haensler, A., Hempelmann, N., Jones, C., Keuler, K., Kovats, S., Kröner, N., Kotlarski, S., Kriegsmann, A., Martin, E., van Meijgaard, E., Moseley, C., Pfeifer, S., Preuschmann, S., Radermacher, C., Radtke, K., Rechid, D., Rounsevell, M., Samuelsson, P., Somot, S., Soussana, J.-F., Teichmann, C., Valentini, R., Vautard, R., Weber, B., and Yiou, P.: EURO-CORDEX: new high-resolution climate change projections for  
635 European impact research, *REG ENVIRON CHANGE*, 14, 563-578, <https://doi.org/10.1007/s10113-013-0499-2>, 2014.
- Johannsen, L. L., Schmaltz, E. M., Mitrovits, O., Klik, A., Smoliner, W., Wang, S., and Strauss, P.: An update of the spatial and temporal variability of rainfall erosivity (R-factor) for the main agricultural production zones of Austria, *CATENA*, 215, 106305, <https://doi.org/10.1016/j.catena.2022.106305>, 2022.
- Kendon, E. J., Roberts, N. M., Fowler, H. J., Roberts, M. J., Chan, S. C., and Senior, C. A.: Heavier summer downpours with  
640 climate change revealed by weather forecast resolution model, *NAT CLIM CHANGE*, 4, 570-576, <https://doi.org/10.1038/nclimate2258>, 2014.
- Kendon, E. J., Ban, N., Roberts, N. M., Fowler, H. J., Roberts, M. J., Chan, S. C., Evans, J. P., Fosser, G., and Wilkinson, J. M.: Do convection-permitting regional climate models improve projections of future precipitation change?, *B AM METEOROL SOC*, 98, 79-93, <https://doi.org/10.1175/BAMS-D-15-0004.1>, 2017.
- 645 Kharin, V. V., Zwiers, F. W., Zhang, X., and Wehner, M.: Changes in temperature and precipitation extremes in the CMIP5 ensemble, *CLIMATIC CHANGE*, 119, 345-357, <https://doi.org/10.1007/s10584-013-0705-8>, 2013.
- Kirkby, M., Irvine, B. J., Jones, R., Govers, G., and the PESERA team: The PESERA coarse scale erosion model for Europe . I. – Model rationale and implementation, *EUR J SOIL SCI*, 59, 1293-1306, 2008.
- Kondolf, G. M., Gao, Y., Annandale, G. W., Morris, G. L., Jiang, E., Zhang, J., Cao, Y., Carling, P., Fu, K., Guo, Q., Hotchkiss,  
650 R., Peteuil, C., Sumi, T., Wang, H. W., Wang, Z., Wei, Z., Wu, B., Wu, C., and Yang, C. T.: Sustainable sediment management in reservoirs and regulated rivers: experiences from five continents, *EARTHS FUTURE*, 2, 256-280, <https://doi.org/10.1002/2013EF000184>, 2014.
- Kreklow, J., Steinhoff-Knopp, B., Friedrich, K., and Tetzlaff, B.: Comparing rainfall erosivity estimation methods using weather radar data for the State of Hesse (Germany), *WATER-SUI*, 12, 1424, <https://doi.org/10.3390/w12051424>, 2020.
- 655 Laflen, J. M., Lane, L. J., and Foster, G. R.: WEPP: A new generation of erosion prediction technology, *J SOIL WATER CONSERV*, 46, 34-38, 1991.



- McCool, D. K., Foster, G. R., Mutchler, C. K., and Meyer, L. D.: Revised slope length factor for the Universal Soil Loss Equation, *T ASAE*, 32, 1571-1576, 1989.
- Meusburger, K., Steel, A., Panagos, P., Montanarella, L., and Alewell, C.: Spatial and temporal variability of rainfall erosivity factor for Switzerland, *HYDROL EARTH SYST SC*, 16, 167-177, <https://doi.org/10.5194/hess-16-167-2012>, 2012.
- 660 Morgan, R. and Duzant, J.: Modified MMF (Morgan–Morgan–Finney) model for evaluating effects of crops and vegetation cover on soil erosion, *EARTH SURF PROC LAND*, 33, 90-106, <https://doi.org/10.1002/esp.1530>, 2008.
- Morgan, R., Morgan, D., and Finney, H.: A predictive model for the assessment of soil erosion risk, *J AGR ENG RES*, 30, 245-253, [https://doi.org/10.1016/S0021-8634\(84\)80025-6](https://doi.org/10.1016/S0021-8634(84)80025-6), 1984.
- 665 Mueller, E. N. and Pfister, A.: Increasing occurrence of high-intensity rainstorm events relevant for the generation of soil erosion in a temperate lowland region in Central Europe, *J HYDROL*, 411, 266-278, <https://doi.org/10.1016/j.jhydrol.2011.10.005>, 2011.
- Mueller, M., Bierschenk, A. M., Bierschenk, B. M., Pander, J., and Geist, J.: Effects of multiple stressors on the distribution of fish communities in 203 headwater streams of Rhine, Elbe and Danube, *SCI TOTAL ENVIRON*, 703, 134523, <https://doi.org/10.1016/j.scitotenv.2019.134523>, 2020.
- 670 Nearing, M. A., Pruski, F. F., and O'Neal, M. R.: Expected climate change impacts on soil erosion rates: A review, *J SOIL WATER CONSERV*, 59, 43--50, 2004.
- Nearing, M. A., Yin, S.-q., Borrelli, P., and Polyakov, V. O.: Rainfall erosivity: An historical review, *CATENA*, 157, 357-362, <https://doi.org/10.1016/j.catena.2017.06.004>, 2017.
- 675 Nord, G. and Esteves, M.: PSEM\_2D: A physically based model of erosion processes at the plot scale, *WATER RESOUR RES*, 41, <https://doi.org/10.1029/2004WR003690>, 2005.
- Orgiazzi, A. and Panagos, P.: Soil biodiversity and soil erosion: It is time to get married: Adding an earthworm factor to soil erosion modelling, *GLOBAL ECOL BIOGEOGR*, 27, 1155-1167, <https://doi.org/10.1111/geb.12782>, 2018.
- OSPAR Commission: Eutrophication status of the OSPAR maritime area. Third integrated report on the eutrophication status of the OSPAR maritime area, OSPAR Commission, London, United Kingdom, 166 pp., 2017.
- 680 Owens, P. N., Batalla, R. J., Collins, A. J., Gomez, B., Hicks, D. M., Horowitz, A. J., Kondolf, G. M., Marden, M., Page, M. J., Peacock, D. H., Petticrew, E. L., Salomons, W., and Trustrum, N. A.: Fine-grained sediment in river systems: Environmental significance and management issues, *RIVER RES APPL*, 21, 693-717, <https://doi.org/10.1002/rra.878>, 2005.
- Panagos, P., Meusburger, K., Ballabio, C., Borrelli, P., and Alewell, C.: Soil erodibility in Europe: A high-resolution dataset based on LUCAS, *SCI TOTAL ENVIRON*, 479, 189-200, <https://doi.org/10.1016/j.scitotenv.2014.02.010>, 2014.
- 685 Panagos, P., Ballabio, C., Borrelli, P., Meusburger, K., Klik, A., Rousseva, S., Tadić, M. P., Michaelides, S., Hrabalíková, M., and Olsen, P.: Rainfall erosivity in Europe, *SCI TOTAL ENVIRON*, 511, 801-814, <https://doi.org/10.1016/j.scitotenv.2015.01.008>, 2015c.



- 690 Panagos, P., Borrelli, P., Meusburger, K., Alewell, C., Lugato, E., and Montanarella, L.: Estimating the soil erosion cover-  
management factor at the European scale, *LAND USE POLICY*, 48, 38-50, <https://doi.org/10.1016/j.landusepol.2015.05.021>,  
2015a.
- Panagos, P., Borrelli, P., Poesen, J., Ballabio, C., Lugato, E., Meusburger, K., Montanarella, L., and Alewell, C.: The new  
assessment of soil loss by water erosion in Europe, *ENVIRON SCI POLICY*, 54, 438-447,  
<https://doi.org/10.1016/j.envsci.2015.08.012>, 2015b.
- 695 Panagos, P., Ballabio, C., Meusburger, K., Spinoni, J., Alewell, C., and Borrelli, P.: Towards estimates of future rainfall  
erosivity in Europe based on REDES and WorldClim datasets, *J HYDROL*, 548, 251-262,  
<https://doi.org/10.1016/j.jhydrol.2017.03.006>, 2017.
- Panagos, P., Borrelli, P., Matthews, F., Liakos, L., Bezak, N., Diodato, N., and Ballabio, C.: Global rainfall erosivity  
projections for 2050 and 2070, *J HYDROL*, 610, 127865, <https://doi.org/10.1016/j.jhydrol.2022.127865>, 2022.
- 700 Pham, T. V., Steger, C., Rockel, B., Keuler, K., Kirchner, I., Mertens, M., Rieger, D., Günther, Z., and Früh, B.: ICON in  
Climate Limited-area Mode (ICON release version 2.6. 1): A new regional climate model, *GEOSCI MODEL DEV*, 14, 985-  
1005, <https://doi.org/10.5194/gmd-14-985-2021>, 2021.
- Phinzi, K. and Ngetar, N. S.: The assessment of water-borne erosion at catchment level using GIS-based RUSLE and remote  
sensing: A review, *International Soil and Water Conservation Research*, 7, 27-46, <https://doi.org/10.1016/j.iswcr.2018.12.002>,  
705 2019.
- Pierce, D.: Package ‘ncdf4’ [code], 2019.
- Pimentel, D., Harvey, C., Resosudarmo, P., Sinclair, K., Kurz, D., McNair, M., Crist, S., Shpritz, L., Fitton, L., and Saffouri,  
R.: Environmental and economic costs of soil erosion and conservation benefits, *SCIENCE*, 267, 1117-1123,  
<https://doi.org/10.1126/science.267.5201.1117>, 1995.
- 710 Pohlert, T.: Projected climate change impact on soil erosion and sediment yield in the river Elbe catchment, in: *Sediment  
Matters*, edited by: Heininger, P., Cullmann, J., Springer, Cham., 97-108, [https://doi.org/10.1007/978-3-319-14696-6\\_7](https://doi.org/10.1007/978-3-319-14696-6_7), 2015.
- Prein, A. F., Langhans, W., Fosser, G., Ferrone, A., Ban, N., Goergen, K., Keller, M., Tölle, M., Gutjahr, O., Feser, F., Brisson,  
E., Kollet, S., Schmidli, J., van Lipzig, N. P. M., and Leung, R.: A review on regional convection-permitting climate modeling:  
Demonstrations, prospects, and challenges, *REV GEOPHYS*, 53, 323-361, <https://doi.org/10.1002/2014RG000475>, 2015.
- 715 Quine, T. A. and Van Oost, K.: Insights into the future of soil erosion, *Proceedings of the National Academy of Sciences*, 117,  
23205-23207, <https://doi.org/10.1073/pnas.2017314117>, 2020.
- Raffa, M., Reder, A., Adinolfi, M., and Mercogliano, P.: A comparison between one-step and two-step nesting strategy in the  
dynamical downscaling of regional climate model COSMO-CLM at 2.2 km driven by ERA5 reanalysis, *ATMOSPHERE-  
BASEL*, 12, 260, <https://doi.org/10.3390/atmos12020260>, 2021.
- 720 Renard, K. G., Foster, G. R., Weesies, G. A., McCool, D. K., and Yoder, D. C.: Predicting soil erosion by water: A guide to  
conservation planning with the Revised Universal Soil Loss Equation (RUSLE), *Agriculture handbook*, 703, 1993.



- Risal, A., Lim, K. J., Bhattarai, R., Yang, J. E., Noh, H., Pathak, R., and Kim, J.: Development of web-based WERM-S module for estimating spatially distributed rainfall erosivity index (EI30) using RADAR rainfall data, *CATENA*, 161, 37-49, <https://doi.org/10.1016/j.catena.2017.10.015>, 2018.
- 725 Ritz, S. and Fischer, H.: A mass balance of nitrogen in a large lowland river (Elbe, Germany), *WATER-SUI*, 11, 2383, <https://doi.org/10.3390/w11112383>, 2019.
- Rockel, B., Will, A., and Hense, A.: The regional climate model COSMO-CLM (CCLM), *METEOROL Z*, 17, 347, <https://doi.org/10.1127/0941-2948/2008/0309>, 2008.
- Rogler, H. and Schwertmann, U.: Erosivität der Niederschläge und Isoerodentkarte Bayerns, *Zeitung für Kulturtechnik und*  
730 *Flurbereinigung*, 22, 99-112, 1981.
- Routschek, A., Schmidt, J., and Kreienkamp, F.: Climate Change impacts on soil erosion: A high-resolution projection on catchment scale until 2100, in *Engineering Geology for Society and Territory - Volume 1*, edited by: Lollino, G., Manconi, A., Clague, J., Shan, W., Chiarle, M., Springer, Cham., 135–141, [https://doi.org/10.1007/978-3-319-09300-0\\_26](https://doi.org/10.1007/978-3-319-09300-0_26), 2015.
- Rybka, H., Haller, M., Brienens, S., Brauch, J., Früh, B., Junghänel, T., Lengfeld, K., Walter, A., and Winterrath, T.:  
735 Convection-permitting climate simulations with COSMO-CLM for Germany: Analysis of present and future daily and sub-daily extreme precipitation, development, *METEOROL Z* 64, 65, <https://doi.org/10.1127/metz/2022/1147>, 2022.
- Sartori, M., Philippidis, G., Ferrari, E., Borrelli, P., Lugato, E., Montanarella, L., and Panagos, P.: A linkage between the biophysical and the economic: Assessing the global market impacts of soil erosion, *LAND USE POLICY*, 86, 299-312, <https://doi.org/10.1016/j.landusepol.2019.05.014>, 2019.
- 740 Schulzweida, U.: CDO User Guide (2.1.0), Zenodo [code], <https://doi.org/10.5281/zenodo.7112925>, 2022.
- Schöl, A., Hein, B., Wyrwa, J., and Kirchesch, V.: Modelling water quality in the Elbe and its estuary-Large scale and long term applications with focus on the oxygen budget of the estuary, *Die Küste*, 81, 203-232, 2014.
- Scoccimarro, E., Gualdi, S., Bellucci, A., Zampieri, M., and Navarra, A.: Heavy precipitation events in a warmer climate: Results from CMIP5 models, *J CLIMATE*, 26, 7902-7911, <https://doi.org/10.1175/JCLI-D-12-00850.1>, 2013.
- 745 Simonneaux, V., Cheggour, A., Deschamps, C., Mouillot, F., Cerdan, O., and Le Bissonnais, Y.: Land use and climate change effects on soil erosion in a semi-arid mountainous watershed (High Atlas, Morocco), *J ARID ENVIRON*, 122, 64-75, <https://doi.org/10.1016/j.jaridenv.2015.06.002>, 2015.
- Slingo, J., Bates, P., Bauer, P., Belcher, S., Palmer, T., Stephens, G., Stevens, B., Stocker, T., and Teutsch, G.: Ambitious partnership needed for reliable climate prediction, *NAT CLIM CHANGE*, 12, 499-503, [https://doi.org/10.1038/s41558-022-  
750 \*01384-8\*, 2022.](https://doi.org/10.1038/s41558-022-01384-8)
- Stefanidis, S., Alexandridis, V., and Ghosal, K.: Assessment of water-induced soil erosion as a threat to Natura 2000 protected areas in Crete Island, Greece, *SUSTAINABILITY-BASEL*, 14, 2738, <https://doi.org/10.3390/su14052738>, 2022.
- Steppeler, J., G., D., Schättler, U., Bitzer, H. W., Gassmann, A., Damrath, U., and Gregoric, G.: Meso-gamma scale forecasts using the nonhydrostatic model LM, *METEOROL ATMOS PHYS*, 82, 75-96, <https://doi.org/10.1007/s00703-001-0592-9>,  
755 2003.



- Sun, Y., Solomon, S., Dai, A., and Portmann, R. W.: How often will it rain?, *J CLIMATE*, 20, 4801-4818, <https://doi.org/10.1175/JCLI4263.1>, 2007.
- Teng, H., Ma, Z., Chappell, A., Shi, Z., Liang, Z., and Yu, W.: Improving rainfall erosivity estimates using merged TRMM and gauge data, *REMOTE SENS-BASEL*, 9, 1134, <https://doi.org/10.3390/rs9111134>, 2017.
- 760 Sørland, S. L., Brogli, R., Pothapakula, P. K., Russo, E., Van de Walle, J., Ahrens, B., Anders, I., Buchignani, E., Davin, E. L., Demory, M.-E., Dosio, A., Feldmann, H., Früh, B., Geyer, B., Keuler, K., Lee, D., Li, D., van Lipzig, N. P. M., Min, S.-K., Panitz, H.-J., Rockel, B., Schär, C., Steger, C., and Thiery, W.: COSMO-CLM regional climate simulations in the Coordinated Regional Climate Downscaling Experiment (CORDEX) framework: a review, *GEOSCI MODEL DEV*, 14, 5125–5154, <https://doi.org/10.5194/gmd-14-5125-2021>, 2021.
- 765 Trambly, Y., Neppel, L., Carreau, J., and Sanchez-Gomez, E.: Extreme value modelling of daily areal rainfall over Mediterranean catchments in a changing climate, *HYDROL PROCESS*, 26, 3934-3944, 2012.
- Uber, M., Rössler, O., Astor, B., Hoffmann, T., Van Oost, K., and Hillebrand, G.: Climate change impacts on soil erosion and sediment delivery to German federal waterways: A case study of the Elbe basin, *ATMOSPHERE-BASEL*, 13, 1752, <https://doi.org/10.3390/atmos13111752>, 2022.
- 770 Uber, M., Haller, M., Brendel, C., Hillebrand, G., and Hoffmann, T.: Past, present and future rainfall erosivity in Central Europe, version 1.0 [dataset], <https://doi.org/10.5281/zenodo.7628957>, 2023.
- Uppala, S. M., Kållberg, P. W., Simmons, A. J., Andrae, U., Da Costa Bechtold, V., Fiorino, M., Gibson, J. K., Haseler, J., Hernandez, A., Kelly, G. A., Li, X., Onogi, K., Saarinen, S., Sokka, N., Allan, R. P., Andersson, E., Arpe, K., Balmaseda, M. A., Beljaars, A. C. M., Van De Berg, L., Bidlot, J., Bormann, N., Caires, S., Chevallier, F.,
- 775 Dethof, A., Dragosavac, M., Fisher, M., Fuentes, M., Hagemann, S., Hólm, E., Hoskins, B. J., Isaksen, I., Janssen, P. A. E. M., Jenne, R., McNally, A. P., Mahfouf, J.-F., Morcrette, J.-J., Rayner, N. A., Saunders, R. W., Simon, P., Sterl, A., Trenberth, K. E., Untch, A., Vasiljevic, D., Viterbo, P., and Woollen, J.: The ERA-40 re-analysis, *Q J ROY METEOR SOC*, 131, 2961-3012, <https://doi.org/10.1256/qj.04.176>, 2005.
- USDA Agricultural Research Service: User's reference guide. Revised Universal Soil Loss Equation version 2 (RUSLE2),
- 780 Documentation, 444 pp., 2008.
- Van Dijk, A., Bruijnzeel, L., and Rosewell, C.: Rainfall intensity–kinetic energy relationships: A critical literature appraisal, *J HYDROL*, 261, 1-23, [https://doi.org/10.1016/S0022-1694\(02\)00020-3](https://doi.org/10.1016/S0022-1694(02)00020-3), 2002.
- Van Oost, K., Govers, G., and Desmet, P.: Evaluating the effects of changes in landscape structure on soil erosion by water and tillage, *LANDSCAPE ECOL*, 15, 577-589, <https://doi.org/10.1023/A:1008198215674>, 2000.
- 785 Van Rompaey, A. J. J., Verstraeten, G., Van Oost, K., Govers, G., and Poesen, J.: Modelling mean annual sediment yield using a distributed approach, *EARTH SURF PROC LAND*, 26, 1221-1236, <https://doi.org/10.1002/esp.275>, 2001.
- Verstraeten, G., Van Oost, K., Van Rompaey, A., Poesen, J., and Govers, G.: Evaluating an integrated approach to catchment management to reduce soil loss and sediment pollution through modelling, *SOIL USE MANAGE*, 18, 386-394, <https://doi.org/10.1111/j.1475-2743.2002.tb00257.x>, 2002.



- 790 Verstraeten, G., Poesen, J., Demarée, G., and Salles, C.: Long-term (105 years) variability in rain erosivity as derived from 10-min rainfall depth data for Ukkel (Brussels, Belgium): Implications for assessing soil erosion rates, *J GEOPHYS RES-ATMOS*, 111, D22109, <https://doi.org/10.1029/2006JD007169>, 2006.
- Vrieling, A., Sterk, G., and de Jong, S. M.: Satellite-based estimation of rainfall erosivity for Africa, *J HYDROL*, 395, 235-241, <https://doi.org/10.1016/j.jhydrol.2010.10.035>, 2010.
- 795 Wang, L., Cherkauer, K. A., and Flanagan, D. C.: Impacts of climate change on soil erosion in the Great Lakes region, *WATER-SUI*, 10, 715, <https://doi.org/10.3390/w10060715>, 2018.
- Watanabe, M., Suzuki, T., O'ishi, R., Komuro, Y., Watanabe, S., Emori, S., Takemura, T., Chikira, M., Ogura, T., Sekiguchi, M., and et al.: Improved climate simulation by MIROC5: mean states, variability, and climate sensitivity, *J CLIMATE*, 23, 6312-6335, <https://doi.org/10.1175/2010JCLI3679.1>, 2010.
- 800 Westra, S., Alexander, L. V., and Zwiers, F. W.: Global increasing trends in annual maximum daily precipitation, *J CLIMATE*, 26, 3904-3918, <https://doi.org/10.1029/2009JD012008>, 2013.
- Westra, S., Fowler, H. J., Evans, J. P., Alexander, L. V., Berg, P., Johnson, F., Kendon, E. J., Lenderink, G., and Roberts, N.: Future changes to the intensity and frequency of short-duration extreme rainfall, *REV GEOPHYS*, 52, 522-555, <https://doi.org/10.1002/2014RG000464>, 2014.
- 805 Wilken, F., Baur, M., Sommer, M., Deumlich, D., Bens, O., and Fiener, P.: Uncertainties in rainfall kinetic energy-intensity relations for soil erosion modelling, *CATENA*, 171, 234-244, <https://doi.org/10.1016/j.catena.2018.07.002>, 2018.
- Williams, J.: The EPIC model, in: Computer models of watershed hydrology, edited by: Singh, V.P., Water Resources Publications, Highlands Ranch, USA, 909-1000, 1995.
- Williams, J. and Berndt, H.: Sediment yield prediction based on watershed hydrology, *T ASAE*, 20, 1100-1104, 1977.
- 810 Williams, J., Renard, K., and Dyke, P.: EPIC: A new method for assessing erosion's effect on soil productivity, *J SOIL WATER CONSERV*, 38, 381-383, 1983.
- Wischmeier, W. H.: A rainfall erosion index for a universal soil-loss equation, *SOIL SCI SOC AM J*, 23, 246-249, 1959.
- Wischmeier, W. H. and Smith, D. D.: Rainfall energy and its relationship to soil loss, *Eos, Transactions American Geophysical Union*, 39, 285-291, <https://doi.org/10.1029/TR039i002p00285>, 1958.
- 815 Wischmeier, W. H. and Smith, D. D.: Predicting rainfall erosion losses-a guide to conservation planning, United States Department of Agriculture, Agriculture Handbook No. 537, 58 pp., 1978.
- Wisser, D., Frolking, S., Hagen, S., and Bierkens, M. F. P.: Beyond peak reservoir storage? A global estimate of declining water storage capacity in large reservoirs, *WATER RESOUR RES*, 49, 5732-5739, <https://doi.org/10.1002/wrcr.20452>, 2013.
- Yin, S., Xie, Y., Nearing, M., and Wang, C.: Estimation of rainfall erosivity using 5-to 60-minute fixed-interval rainfall data from China, *CATENA*, 70, 306-312, <https://doi.org/10.1016/j.catena.2006.10.011>, 2007.
- 820 Zhao, G., Mu, X., Wen, Z., Wang, F., and Gao, P.: Soil erosion, conservation, and eco-environment changes in the Loess Plateau of China, *LAND DEGRAD DEV*, 24, 499-510, <https://doi.org/10.1002/ldr.2246>, 2013.